CellPress
Partner Journal

Molecular Plant
Research Article

Cell-specific pathways recruited for symbiotic nodulation in the *Medicago truncatula* legume

Sergio Alan Cervantes-Pérez[1,5], Sandra Thibivilliers[1,2,5], Carole Laffont[3], Andrew D. Farmer[4], Florian Frugier[3] and Marc Libault[1,2,*]

[1]Department of Agronomy and Horticulture, Center for Plant Science Innovation, University of Nebraska-Lincoln, Lincoln, NE 68503, USA

[2]Single Cell Genomics Core Facility, Center for Biotechnology, University of Nebraska-Lincoln, Lincoln, NE 68588, USA

[3]Institute of Plant Sciences Paris-Saclay (IPS2), Université Paris-Saclay, CNRS, INRAE, Université Paris-Cité, Université d'Evry, 91190 Gif-sur-Yvette, France

[4]National Center for Genome Resources, Santa Fe, NM 87505, USA

[5]These authors contributed equally to this article.

***Correspondence: Marc Libault (marc.libault@unl.edu)**

https://doi.org/10.1016/j.molp.2022.10.021

ABSTRACT

***Medicago truncatula* is a model legume species that has been studied for decades to understand the symbiotic relationship between legumes and soil bacteria collectively named rhizobia. This symbiosis called nodulation is initiated in roots with the infection of root hair cells by the bacteria, as well as the initiation of nodule primordia from root cortical, endodermal, and pericycle cells, leading to the development of a new root organ, the nodule, where bacteria fix and assimilate the atmospheric dinitrogen for the benefit of the plant. Here, we report the isolation and use of the nuclei from mock and rhizobia-inoculated roots for the single nuclei RNA-seq (sNucRNA-seq) profiling to gain a deeper understanding of early responses to rhizobial infection in Medicago roots. A gene expression map of the Medicago root was generated, comprising 25 clusters, which were annotated as specific cell types using 119 Medicago marker genes and orthologs to *Arabidopsis* cell-type marker genes. A focus on root hair, cortex, endodermis, and pericycle cell types, showing the strongest differential regulation in response to a short-term (48 h) rhizobium inoculation, revealed not only known genes and functional pathways, validating the sNucRNA-seq approach, but also numerous novel genes and pathways, allowing a comprehensive analysis of early root symbiotic responses at a cell type-specific level.**

Key words: Medicago root, single-cell transcriptomic, rhizobium, nodule initiation, root hair cells, cortical cells

Cervantes-Pérez S.A., Thibivilliers S., Laffont C., Farmer A.D., Frugier F., and Libault M. (2022). Cell-specific pathways recruited for symbiotic nodulation in the *Medicago truncatula* legume. Mol. Plant. **15**, 1868–1888.

INTRODUCTION

Legumes symbiotically interact with nitrogen-fixing soil bacteria collectively named rhizobia. The molecular, physiological, and cellular responses of this symbiosis named nodulation have been extensively studied over the past decades (Roy et al., 2019). Legume nodulation is a complex biological process that requires the activation of temporally and spatially coordinated programs in a limited number of root cells. Briefly, legume nodulation is initiated by the perception of the rhizobial lipochitooligosaccharide Nod factors (NFs) and the subsequent infection of plant root hair cells by rhizobia. Concomitantly, a nodule primordium emerges. In *Medicago truncatula*, a legume species generating indeterminate nodules, these primordia are initiated from cell divisions within the root inner cortex, endodermis, and pericycle layers, and an apical meristem is then established and maintained during the entire life of the nodule. Rhizobia infect the developing root nodule primordia, differentiate into bacteroids, and fix and assimilate the atmospheric dinitrogen allowing a steady supply of nitrogen for the plant.

Functional genomic studies revealed the role of many legume genes controlling the early stages of nodulation, notably in root hair cells (trichoblasts) where the initial microsymbiont perception and the rhizobial infection take place, but also to a lower extent in pericycle and cortex inner root cell layers where nodule organogenesis initiates (Roy et al., 2019). Several *M.truncatula* genes have been functionally characterized to control the infection of the root epidermis. Among them, Nodule Pectate Lyase (*MtNPL*) (Xie et al., 2012), a gene encoding a cell wall degrading enzyme required for the initiation of infection threads in curled root hairs, Lumpy Infections (*MtLIN*) (Kiss et al., 2009; Liu et al., 2019a),

Published by the Molecular Plant Shanghai Editorial Office in association with Cell Press, an imprint of Elsevier Inc., on behalf of CSPB and CEMPS, CAS.

which encodes a putative E3 ligase, Rhizobium Directed Polar Growth (*MtRPG)* (Arrighi et al., 2008)], a gene encoding a protein with a coiled-coiled domain, *MtFLOT4* (Haney and Long, 2010), *MtVPY* (Murray et al., 2011), NADPH oxidase/respiratory burst oxidase homologs (e.g., Rboh) (Montiel et al., 2016), and *MtCBS1*, a gene encoding a Cystathionine-β-Synthase-like Domain-Containing Protein (Sinharoy et al., 2016), are all upregulated in response to rhizobium inoculation. In addition, other rhizobium-upregulated genes participate in the NF signaling pathway, such as LYsM receptors that perceive NF bacterial signals. These genes belong to the LysM receptor kinase and LYK-related gene families (*MtLYK* and *MtLYR*, respectively; e.g., *MtNFP* [NF Perception]) (Gough et al., 2018), Does not Make Infections (*MtDMI1, 2 and 3*) genes (Endre et al., 2002; Ané et al., 2004; Gleason et al., 2006), Plant U-box protein 1 and 2 (*MtPUB1 and 2*) involved in protein degradation (Mbengue et al., 2010; Liu et al., 2018) NF Hydrolase 1 (*MtNFH1)* (Cai et al., 2018), which controls NF degradation, Interacting with DMI3 (*MtIPD3)* (Messinese et al., 2007)], and various transcription factor (TF) genes (e.g., Nodulation Signaling Pathway 1/2 [*MtNSP1*] [Kaló et al., 2005; Smit et al., 2005], Nuclear factor-YA1 [*MtNF-YA1]* [Combier et al., 2006], Ethylene Response Factor [*MtERN1]* Required for Nodulation [Andriankaja et al., 2007; Middleton et al., 2007], and *MtNIN* [Nodule Inception] [Schauser et al., 1999]).

To date, a limited number of studies have highlighted the regulatory mechanisms controlling the response of inner root cell layers to rhizobial inoculation (i.e., pericycle, endodermis, and cortex). Among them, cytokinin signaling is necessary and sufficient to promote the initiation of nodule primordia and inhibit the response of epidermal root cells to rhizobia and NFs (Gonzalez-Rizzo et al., 2006; Murray et al., 2007; Plet et al., 2011; Boivin et al., 2016; Jardinaud et al., 2016; Gamas et al., 2017; Lin et al., 2021). Genes controlling root development were also shown to be recruited for nodule development, such as *MtPLT* (Plethora) (Franssen et al., 2015), Knotted homeobox (*MtKNOX)* (Di Giacomo et al., 2017), LOB Binding Domain 16 (*MtLBD16)* (Schiessl et al., 2019; Soyano et al., 2019), ShortRoot (*MtSHR)* (Dong et al., 2021), Scarecrow (*MtSCR)* (Dong et al., 2021), and *MtNOOT1* (Shen et al., 2019). On some occasions, genes were shown to have a dual function to promote root epidermal infection and nodule initiation at the level of the pericycle and cortical cells, such as *MtNIN* (Liu et al., 2019b).

To gain a more accurate picture of the symbiotic transcriptional programs controlling the root hair signal perception and infection, transcriptomic studies were conducted on populations of isolated legume root hair cells using root hair shaving or laser dissection (Libault et al., 2009; Breakspear et al., 2014). Similarly, -omics analyses targeting the zone of emerging nodules revealed the transcriptomic programs controlling the initiation and development of nodule primordia (Lohar et al., 2005; Larrainzar et al., 2015; van Zeijl et al., 2015; Schiessl et al., 2019). While valuable, these approaches suffer from the cellular heterogeneity of the isolated root hair populations (i.e., a mixture of unresponsive, responsive but uninfected, and infected root hair cells) (Bhuvaneswari et al., 1981), and from the cellular complexity of the root. For instance, as a reflection of the cellular heterogeneity of the root hair population, it has been estimated that only 1%–5% of the root hair cells are infected by rhizobia (Nutman, 1959).

While these approaches increased the resolution of plant transcriptomic analyses, they have been recently superseded by the emergence of single-cell RNA sequencing (scRNA-seq) and single-nucleus RNA-seq (sNucRNA-seq) transcriptomic technologies. Here, we report the use of the sNucRNA-seq technology on *M.truncatula* roots mock-inoculated or inoculated with its symbiont, *Ensifer (Sinorhizobium) meliloti*, to precisely capture the transcriptomic programs induced during the early stages of the nodulation process in each cell type composing the *M.truncatula* root. The establishment of a single-cell resolution transcriptomic map of the *M.truncatula* root allowed for the characterizing of the transcriptomic response of the *M.truncatula* root hair, cortical, endodermal, and pericycle cells at an early stage (48 h) after *E. meliloti* inoculation. The transcriptomic analysis of these different cell types revealed the dynamic regulation of *M.truncatula* genes in response to rhizobial infection, including many novel genes and functional pathways, as well as the differential recruitment of previously known nodulation-related and hormonal genes depending on cell types.

RESULTS

Establishment of a transcriptional map of the rhizobium-inoculated *M. truncatula* root at a single-cell resolution

Isolated plant protoplasts and nuclei have been successfully used to establish single-cell resolution transcriptomes notably from Arabidopsis root cells (Denyer et al., 2019; Jean-Baptiste et al., 2019; Ryu et al., 2019; Shulse et al., 2019; Zhang et al., 2019; Farmer et al., 2021). The high correlation between cellular, nuclear, and whole root transcriptomes (Farmer et al., 2021) supports the biological relevance of both scRNA-seq and sNucRNA-seq approaches. However, the nuclear-based transcriptomic technology has unique advantages compared with the protoplast-based transcriptomic technology, including the ease of nuclei isolation from various plant species and organs, and the limited induction of stress-related genes (i.e., in contrast, protoplastization leads to the induction of hundreds of stress-responsive genes) (Birnbaum et al., 2003; Denyer et al., 2019). Therefore, we conducted sNucRNA-seq experiments to characterize the transcriptomic profiles of the different cell-types composing the Medicago root apex and their early response to rhizobial inoculation.

Shortly, Medicago seedlings were inoculated 4 days aftergermination with water or a bacterial suspension of *E. meliloti* (OD_{600nm} = 0.1). Forty-eight hours after rhizobium inoculation, root tips including fully elongated root hair cells were collected and committed to nuclei isolation (see methods for details). Three independent *E. meliloti*-inoculated and three independent mock-inoculated sNucRNA-seq libraries were generated using the 10× Genomics Chromium platform. To establish transcriptomic profiles of Medicago root cells, we applied a pre-mRNA strategy using Cell Ranger (10× Genomics) to map sequencing reads against transcripts and introns of the v1.8 annotation of the MtrunA17r5.0-ANR genome (Pecrix et al., 2018). This first step was followed by the removal of the ambient transcriptomic noise and the detection and removal of doublets (i.e., two nuclei encapsulated into the same reaction volume) (see methods). To support the quality of the libraries, we analyzed the distribution of the number of expressed genes per nucleus and observed an expected normal distribution (Supplemental

Figure 1). To remove outliers and low-quality nuclei, we applied a 95% confidence interval to the normal distribution of the six integrated libraries (Supplemental Figure 1). Taken together, the transcriptomes of 15 854 *E. meliloti*-inoculated and 12 521 mock-inoculated *M.truncatula* root nuclei were further analyzed (Supplemental Table 1), with a median value of 1,053 expressed genes per nucleus and a total of 31,307 expressed protein-coding genes detected (70.2% of the 44 615 Medicago -protein-coding genes) (Pecrix et al., 2018). Considering that the number of Arabidopsis and Medicago expressed genes per nucleus are similar (i.e., 1,124 expressed genes per Arabidopsis nucleus), the percentage of Medicago protein-coding genes expressed is less compared with Arabidopsis (i.e., 89.4% of 27,420 protein-coding genes) (Farmer et al., 2021). Such a limited percentage might be a consequence of the neo- or sub-functionalization of Medicago genes following the whole-genome duplication that occurred 58 million years ago, or the result of an over-estimation of the number of protein-coding genes in Medicago compared with the reference Arabidopsis genome.

Using the Seurat package, we normalized and integrated 28,375 nuclei transcriptomes before applying the uniform manifold approximation and projection (UMAP) technique to cluster the nuclei according to their transcriptomic profiles. Twenty-five clusters were identified (Figure 1A) the dataset can be interrogated using the https://shinycell.legumeinfo.org/medtr.A17.gnm5.ann1_6.expr.Cervantes-Perez_Thibivilliers_2022/ web interface) (Ouyang et al., 2021), for which the percentage of nuclei per cluster was not statistically different between inoculated and mock-inoculated conditions (Student t-test > 0.05; Figure 1B; Supplemental Table 1). While *E. meliloti* inoculation did not lead to changes in the number of clusters or the overall topography of the UMAP projection, we repetitively noticed a local modification in the distribution of a subpopulation of cluster #2 nuclei (Figure 1A, red circle). These results highlight that the *E. meliloti* inoculation induces significant changes in the transcriptome of these Medicago root cells.

Functional annotation of Medicago root nuclei clusters

The functional annotation of root cells/nuclei according to their transcriptomic profile was previously successfully achieved in the model species *A. thaliana* by exploring the transcriptional pattern of a large number of functionally characterized cell type-specific marker genes (Denyer et al., 2019; Jean-Baptiste et al., 2019; Ryu et al., 2019; Shulse et al., 2019; Zhang et al., 2019; Farmer et al., 2021). To annotate the 25 nuclei clusters of the UMAP, we first analyzed the transcriptional pattern of the few available functionally characterized Medicago root cell type-specific markers (Supplemental Table 2). The *MtPLT1-4* genes are specifically expressed in the quiescent center of the root and nodule primordia (Franssen et al., 2015). Looking at their expression pattern in the Medicago UMAP, they are all preferentially expressed in the central star-shaped cluster #9, supporting its annotation as the stem cell niche cluster (Figures 2A and 2B). To annotate Medicago epidermal cells, the expression of the phosphate transporter *MtPT1* gene, which is specifically expressed in Medicago root hairs and epidermal cells (Chiou et al., 2001), was analyzed. *MtPT1* was mostly expressed in clusters #1 and #2, and to a lesser extent, in cluster #5 (Figure 2B). The root hair-specific *MtRbohF* gene (Marino et al., 2011) was mostly expressed in cluster #3 (Figure 2B), suggesting its annotation as root hair cells. To support the annotation of the root epidermal cells, we also analyzed the expression of 45 genes previously identified as specifically expressed in the root hair (Breakspear et al., 2014) and 25 Medicago genes orthologous to the 168 root hair-specific Arabidopsis genes (Cvrčková et al., 2010). Taken together, most of these genes are preferentially or specifically expressed in the Medicago root epidermal cells (Supplemental Figure 2, red rectangles), especially in cluster #3. Based on the expression pattern of these different Medicago markers, clusters #1 and #2 could be thus confidently annotated as root epidermal cell clusters, and cluster #3 as a root hair cell cluster (Figure 2A). To identify the Medicago cortical cells on the UMAP projection, we analyzed the transcriptional activity of the cortical cell-specific genes *MtIFS1*, *MtIFS3*, and *MtPAL5* (Biala et al., 2017). *MtIFS1* was almost specifically expressed, and *MtIFS3* and *MtPAL5* were preferentially expressed in cluster #14 (Figure 2B). Besides, *MtIFS3* and *MtPAL5* are also detected in clusters #7 and #10, and in clusters #18 and #19, respectively. Taken together, these results support the annotation of cluster #14 as a cortical cell cluster. *MtSCR* is mostly expressed in the endodermis as well as in cortical and epidermal cells (Dong et al., 2021) and was thus used for annotating the endodermis (Figure 2A). *MtSCR* was mostly detected in clusters #17, #18, and #19 that are co-localized on the UMAP projection (Figure 2B), which were thus annotated as endodermal cell clusters. *MtPHO1.1*, *MtPHO1.3*, and to a lesser extent, *MtPHO1.2*, are preferentially expressed in the root stele and more specifically in pericycle cells (Nguyen et al., 2020). *MtPHO1.1* and *MtPHO1.3* were most expressed in cluster #20, where *MtPHO1.2* is also highly expressed, as well as in cluster #5. The transcriptional activity of these three *PHO1* genes supports that cluster #20 is associated with the root pericycle and/or stele (Figure 2A). Other genes expressed in the root stele, such as *MtHext1/STP13*, *MtSHR1*, *MtSHR2*, and *MtPAL* (Gaude et al., 2012; Biala et al., 2017; Dong et al., 2021), were co-expressed in clusters #19–#24 (Figure 2B). Considering that *MtSCR*, an endodermal cell marker gene, is highly expressed in cluster #19, this suggests that clusters #20–#- to 24 correspond with root stele cell types (Figure 2A). Besides, *MtYUC8* and *MtABCG20* genes that are active in the vascular bundle of the Medicago root (Pawela et al., 2019; Schiessl et al., 2019) were mostly expressed in cluster #25 (Figure 2A). Taken together, this supports the annotation of cluster #20 as the Medicago pericycle cell cluster, and of clusters #21–#25 as Medicago root vasculature cell-type clusters. Finally, the expression pattern of *MtSUNN*, a receptor-like kinase acting in the autoregulation of nodulation (AON) pathway specifically expressed in the phloem (Schnabel et al., 2012), precisely maps to cluster #25, thus refining its annotation as the phloem cells cluster, and the *MtRDN1* AON-related enzyme modifying CLE signaling peptides (Kassaw et al., 2017) to cluster #24, thus refining its annotation as a xylem cells cluster (Figure 2A).

Use of Medicago orthologs of *Arabidopsis* root cell-type markers for functional annotation of clusters

To further support the functional annotation of these Medicago root clusters, we additionally analyzed the transcriptional activity of Medicago genes orthologous to 1,086 Arabidopsis root

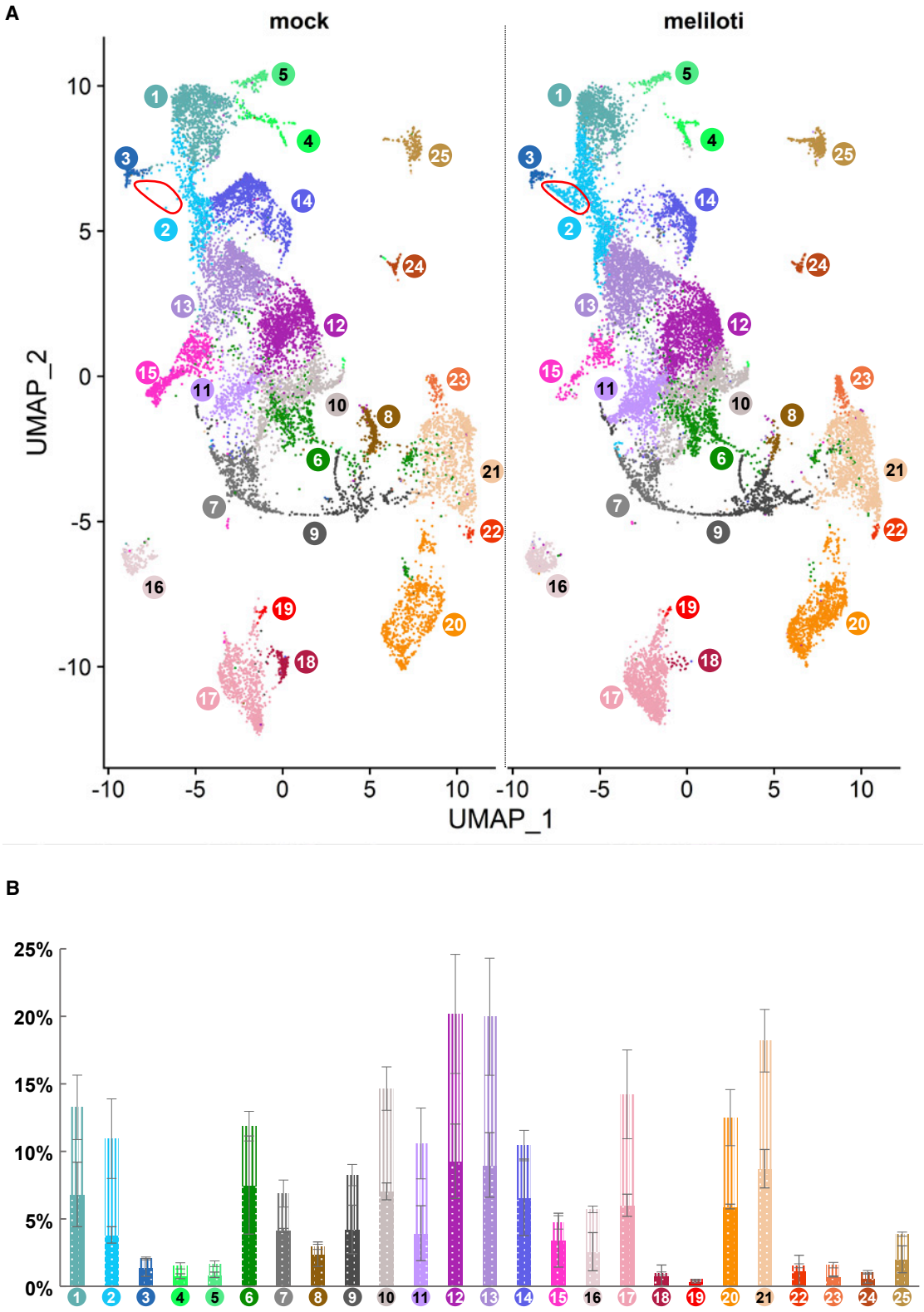

Figure 1. Single-nuclei RNA-seq of the *M. truncatula* roots reveals 25 different root clusters.
(A) UMAP clustering of *M. truncatula*/*E. meliloti*- and mock-inoculated root nuclei according to their transcriptomic profiles. While the overall topography of these two UMAPs is well conserved, subtle differences are observed (e.g., highlighted in red for cluster #2).
(B) Percentage of *E. meliloti* (dash bars) and mock-inoculated (solid bars) nuclei allocated in the 25 clusters composing the *M. truncatula* root UMAP.

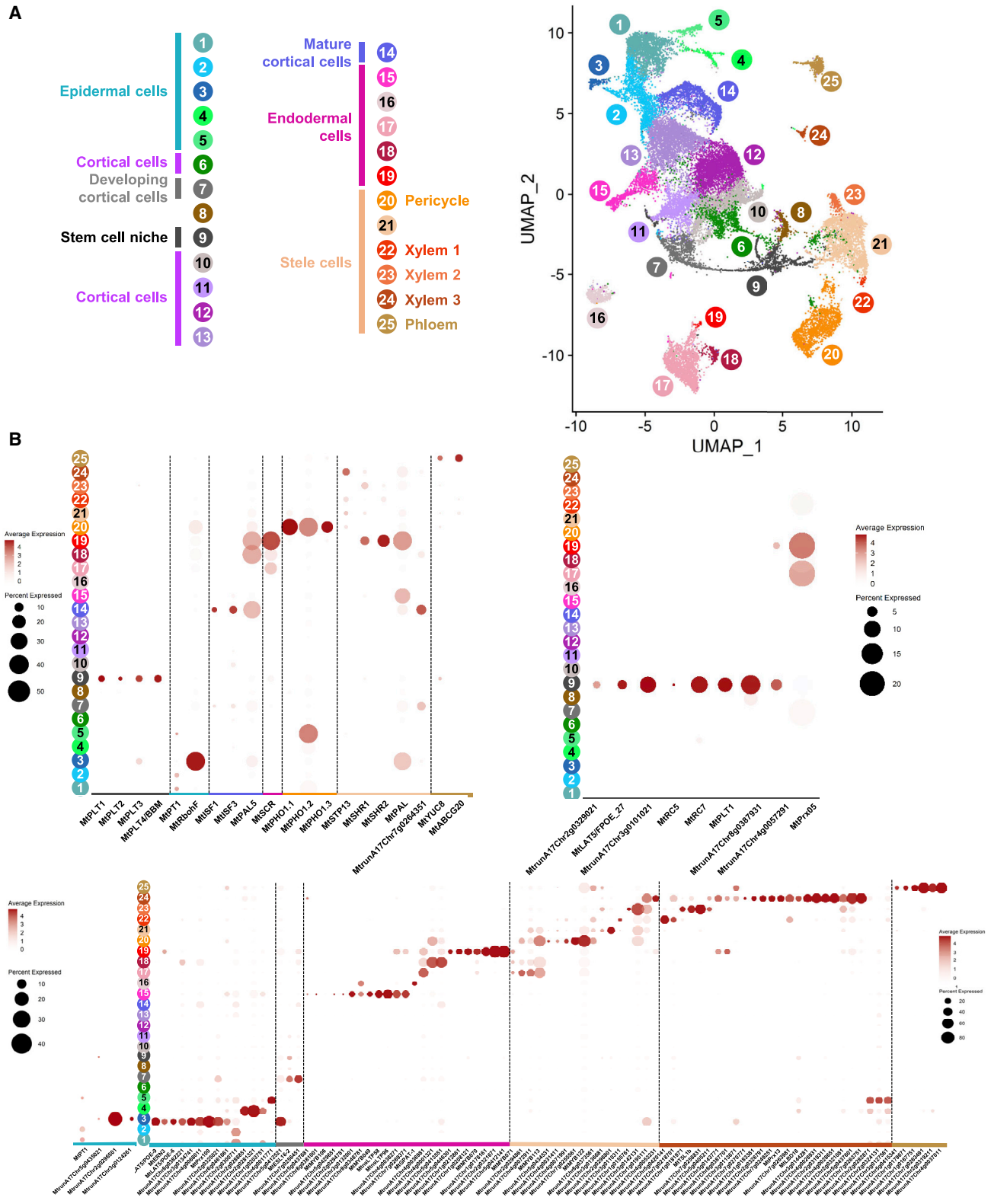

Figure 2. Functional annotation of the 25 *M. truncatula* root clusters.

(A) UMAP clustering and functional annotation of the Medicago root cell-type clusters based on the expression of Medicago marker genes and of genes orthologous to Arabidopsis root marker genes.

(B) Normalized expression levels of cell-type marker genes functionally characterized in Medicago (detailed in Supplemental Table 2), or orthologous to Arabidopsis root cell type-specific marker genes (detailed in Supplemental Table 4) across the 25 Medicago root clusters, shown on the *y* axis. The percentage of nuclei expressing the gene of interest (circle size), and the mean expression (circle color) of genes, are shown for each sub-panel.

cell-type marker genes (Supplemental Table 3), assuming the conservation of their cell-type-specific/-enriched transcriptional patterns. Among these genes, 101 were previously validated markers (Böhme et al., 2004; Fendrych et al., 2014; Olvera-Carrillo et al., 2015; Denyer et al., 2019; Jean-Baptiste et al., 2019; Ryu et al., 2019; Shulse et al., 2019; Turco et al., 2019; Zhang et al., 2019; see Farmer et al., 2021 for an exhaustive list), 324 were identified in at least 2 independent Arabidopsis root single-cell RNA-seq studies (Denyer et al., 2019; Jean-Baptiste et al., 2019; Ryu et al., 2019; Shulse et al., 2019; Zhang et al., 2019), and 868 genes were identified as the most specifically expressed genes within the 21 sNucRNA-seq clusters of the Arabidopsis root (Farmer et al., 2021). We found that 196 Medicago orthologs share microsyntenic relationships with the 1,086 Arabidopsis root cell type-specific marker genes thanks to the Comparative Genomic database (CoGe; https://genomevolution.org/coge/) (Lyons et al., 2008; Lyons and Freeling, 2008). Among these 196 genes, 38 (19.4%) and 58 (29.6%) genes were very low/not expressed, or ubiquitously expressed across all Medicago root clusters, respectively. In the end, we considered 100 Medicago genes orthologous to root cell type-specific Arabidopsis marker genes to annotate Medicago root clusters (Supplemental Table 4).

Among these 100 genes, 10, 2, and 4 are orthologous to Arabidopsis trichoblast-, atrichoblast-, and root cap-specific marker genes, respectively, including the *MtPT1* gene (Chiou et al., 2001) (Supplemental Table 2). Nine trichoblast-specific genes are mostly expressed in cluster #3, whereas *MtPT1* and the remaining six atrichoblast markers are most expressed in clusters #1, #2, #4, and #5 (Figure 2B). This conclusion is further supported by the transcriptional activity in cluster #3 of the *MtLAT52/POE_9* and *MtERN3* genes orthologous to the soybean root hair-specific *Glyma.18G025200* and *Glyma.05G157400/Glyma.08G115000* genes (Qiao et al., 2017), respectively (Figure 2B). Using the same approach, we found that the expression pattern of other Medicago genes orthologous to Arabidopsis cell-type marker genes similarly supported the annotation of the different Medicago root cell-type clusters. The stem cell niche annotation was confirmed for cluster #9 based on the transcriptional activity of nine Medicago genes orthologous to Arabidopsis root meristematic genes (Franssen et al., 2015) (Figure 2B, dark grey). Confirming the expression of the endodermis-specific *MtSCR* gene in clusters #17–#19 (Figure 2B, pink), we additionally identified 23 Medicago genes orthologous to Arabidopsis endodermal cell-specific genes strongly expressed in clusters #15–#19 (Figure 2B, pink). The annotation of clusters #20–#25 as stele cells was also confirmed based on the transcriptional activity of 49 orthologous genes in these clusters. Among them, xylem (i.e., clusters #22, #23, and #24) and phloem cells (i.e., cluster #25) were identified based on the expression of 23 and 6 Medicago genes orthologous to Arabidopsis xylem- and phloem-specific genes, respectively (Figure 2B, brown and light brown). As a note, three genes orthologous to Arabidopsis xylem marker genes (i.e., *MtrunA17Chr2g0282871*, *MtrunA17Chr2g0324131*, and *MtrunA17Chr3g0127561*) were also expressed in clusters #4 and #5. We assume that their activity in these two root epidermal cell clusters could reflect the induction of the cell death program, which was previously reported to be shared between xylem and root cap cells (Kumpf and Nowack, 2015; Heo et al., 2017; Farmer et al., 2021), refining the annotation of clusters #4 and #5 as containing root cap cell types. Finally, the transcriptional activity of three Medicago genes orthologous to Arabidopsis cortical cell-specific genes in cluster #7 (Figure 2B, grey) suggests that it is composed of developing cortical cells. This result is further supported by the activity of the cortical cell-specific *MtIFS3* and *MtPAL5* genes in cluster #7 (Figure 2B, purple).

Taken together, the combined use of previously characterized Medicago root cell-type marker genes with the analysis of the transcriptional activity of Medicago genes orthologous to Arabidopsis root cell-type marker genes led to the functional annotation of 19 out of the 25 Medicago root cell clusters of the UMAP (Figure 2A). To annotate the remaining six clusters (#6, #8, #10, #11, #12, and #13), all located at the center of the UMAP, we conducted a correlation analysis between the different Medicago root cell clusters, hypothesizing that two clusters sharing highly correlated transcriptomic profiles would relate to the same cell type. As expected, this analysis revealed several high correlation scores, such as between the root epidermal clusters #1 and #2, and for stele/pericycle clusters #20, #21, and #23 (Supplemental Figure 3, highlighted in orange and red squares, respectively). As a note, the remaining non-annotated cluster #8 did not share a correlation with any other cluster, suggesting that cells composing this cluster have a very different transcriptomic profile compared with all other clusters. However, we were able to associate cluster #8 with an intense activity of mitochondrial and ribosomal genes (Supplemental Table 5; Supplemental Figure 4). Previous studies linked the high expression of ribosomal genes with plant developmental processes in maize, Arabidopsis, and tobacco plants (Ponnala et al., 2014; Makabe et al., 2017). These results thus suggest that cluster #8 is composed of cells with high biological activity. Interestingly, we found high correlation scores between clusters #6, 7, 10, 11, 12, 13, and 14 (Supplemental Figure 3, yellow squares). As the cell type marker-based analyses identified clusters #7 and #14 as cortical cells, we assume that clusters #6, #10, #11, #12, and #13 are also composed of cortical cells (Figure 2A), potentially at different stages in their differentiation process and/or corresponding to different layers of the cortex, knowing that there are 4–5 layers of cortical cells in *M.truncatula* roots.

Conservation of expression patterns between orthologous *Arabidopsis* and Medicago genes at the single-cell level

The previous Arabidopsis-Medicago comparative genomic and transcriptomic analysis used to annotate Medicago root clusters (Figure 2) suggested that transcriptional patterns of orthologous genes could be largely conserved upon speciation of the 2 plants 108 million years ago (Zeng et al., 2017). To further explore the extent of this conservation at the single-cell level, a correlation analysis was conducted on 3,921 pairs of orthologous genes sharing microsyntenic relationships based on the CoGe database (Lyons et al., 2008; Lyons and Freeling, 2008) (Supplemental Table 6). To maximize the biological significance of the analysis, we processed the previously generated Arabidopsis sNucRNA-seq datasets (Farmer et al., 2021), similarly to the Medicago sNucRNA-seq datasets (see methods). This updated analysis led to the identification and re-annotation of 16 Arabidopsis root clusters (Farmer et al., 2021) (Figure 3A). We observed a similar topology between the Medicago and

Arabidopsis sNucRNA-seq UMAPs (Figures 2A and 3A), with the stem cell niche (#9) located in a star-shaped cluster at the center of the UMAP projection, whereas the most differentiated cell-types (e.g., epidermal [#1, #2, and #3], phloem [#25], xylem cells [#22, #23, and #24]) were retrieved in the periphery. To evaluate the conservation of the transcriptional profiles between Arabidopsis and Medicago orthologs, the average gene transcriptional activity of one-to-one orthologs was similarly calculated for each of the 25 mock-inoculated Medicago (Figure 1A) and of the 16 Arabidopsis root clusters (Figure 3A), and a correlation analysis was then conducted (Figure 3B). Stem cell niche (#9) (Figure 3B, black square) and stele cells (#20–#25) (Figure 3B, peach-orange square) shared the highest correlation between the two species, suggesting that the transcriptional activities of orthologous genes were most conserved across these root cell-types. To a lesser extent, the transcriptomic profiles of orthologous genes were also conserved between the two species in trichoblasts/epidermal root hair cells (#1–#3) (Figure 3B, blue square). Similar conservation was recently reported for root hair, xylem, and phloem cells between the more distantly related rice and Arabidopsis roots (Liu et al., 2021; Zhang et al., 2021). We hypothesize that the unique functions of vascular tissues (xylem and phloem) and trichoblast cells for plant nutrition, as well as the role of the stem cell niche in root development, favored the evolutionary conservation of a core transcriptome between these plant species. In contrast, the transcriptomes of endodermal (#15–#19) and cortical cell types (#6, #7, and #10–#14) were most divergent between Arabidopsis and Medicago (Figure 3B, purple and violet squares), suggesting either a difference in nutrient provision when growing the Arabidopsis and Medicago plants, a lower pressure to maintain the transcriptomic signature of these cell-types between the two species, and/or diverging biological functions of these cell types between Fabaceae (legumes) and Brassicaceae, such as their differential capacity to interact with soil beneficial microbes through endosymbiosis.

A differential transcriptional regulation in response to *E. meliloti* of nodulation and hormonal genes depending on cell types

To date, transcriptomic responses of legume roots to rhizobial inoculation were investigated mainly at the whole root level (Mergaert et al., 2019) or on isolated populations of root hair and epidermal cells (Libault et al., 2009; Breakspear et al., 2014). These bulk analyses, however, lacked resolution, considering that only a subset of plant cells respond to and are infected by rhizobia and that the transcriptional response of cell types located deeper within roots cannot be easily assessed. Here, we had a unique opportunity to explore the differential regulation of gene expression across the different cell types in response to *E. meliloti*.

To estimate the percentage of individual Medicago root epidermal cells responding to *E. meliloti*, we quantified the number of epidermal root cells (i.e., clusters #1, #2, and #3, excluding the epidermal/root cap clusters #4 and #5) expressing typical early rhizobial infection marker genes, namely *MtRPG*, *MtFLOT4*, and *MtVPY* (Roy et al., 2019). In *E. meliloti*-inoculated roots, 19.5% (433/2225 epidermal nuclei) of epidermal nuclei expressed at least one of these symbiotic marker genes, whereas only 2.3% (39/1694 epidermal nuclei) were detected in mock-inoculated roots. The increase in the number of rhizobia-responsive epidermal cells upon *E. meliloti* inoculation identified is, thus, significantly larger than the previously estimated size of the epidermal cells population infected by rhizobia, which was approximately 1%–5% of root hair cells (Nutman, 1959). These results suggest that only a subset of the transcriptionally responsive root epidermal cells from these three clusters is effectively infected by rhizobia.

To identify the set of differentially expressed genes (DEGs) in response to rhizobium inoculation from each Medicago root cell cluster, we used DEsingle, a bioinformatics package designed to identify DEGs from single-cell RNA-seq datasets (Miao et al., 2018). Using a p value threshold of less than 0.05 and a | fold change (FC)| of more than 1.5, we identified a total of 8513 DEGs (Supplemental Table 7). Focusing on the most transcriptionally responsive clusters (i.e., >500 DEGs) (Figure 4A; Supplemental Table 7, bold characters), the root hair cells cluster #2 was retrieved, as well as the cortical clusters #7 and #11, the endodermal clusters #15, #16, and #18, and the pericycle cluster #20. This result nicely fits with knowledge previously gained using microscopy during early nodule ontogeny (Xiao et al., 2014), which showed that cellular symbiotic processes mainly affected epidermal and cortical cells, and to a lesser extent, endodermis and pericycle cells. We thus further focused our analysis on these clusters, as well as on genes previously known to be acting in nodulation and/or previously annotated as related to hormonal pathways regulating early nodulation stages (Roy et al., 2019).

In the trichoblast cluster #2, several known infection-related genes were retrieved as upregulated, namely *MtCBS1*, *MtRbohG*, and *MtRbohH* (Montiel et al., 2018), *MtRPG*, *MtVPY*, and *MtAnn1* (de Carvalho Niebel et al., 1998), and *MtNMN1* (i.e., an ortholog of *GmNMN1*) (Libault et al., 2011). Other genes that belong to the NF signaling pathway were also upregulated in root hair and epidermal cells in response to *E. meliloti*, namely *MtNFH1* and *MtLYK10* (Larrainzar et al., 2015), *MtPUB1* (noting that *MtPUB2* is repressed in this same cluster), *MtIPD3*, *MtDMI1*, *MtDMI2*, *MtDMI3*, *MtNSP1*, *MtNSP2*, *MtERN1*, and *MtERN2* (Cerri et al., 2016), and *MtNIN* (Supplemental Tables 8 and 9, Figure 5). Unexpectedly, *MtKNOX3* and *MtKNOX5* genes, previously proposed to control nodule development (Di Giacomo et al., 2017; Dolgikh et al., 2020), and *Does Not fix Nitrogen 2* (*MtDNF2*) (Bourcy et al., 2013)] and *Nodule Cysteine Rich peptide 112* (*MtNCR112*) (Alunni et al., 2007) genes, regulating later stages of the nodulation process, were also upregulated in cluster #2 48 h after rhizobium inoculation. In addition, we noticed that the *MtNF-YA2* and *MtNF-YA6* genes, phylogenetically related to the early nodulation *MtNF-YA1* gene (Baudin et al., 2015), were also upregulated in cluster #2. Genes belonging to hormonal regulatory pathways were also induced in this cluster in response to rhizobial inoculation. These include notably cytokinin (e.g., *MtIPT1*, *CYP735A1-like*, *MtHPT1*, *MtRRB6*, *MtRRA2*, and *MtRRA5*) (Azarakhsh et al., 2018; Tan et al., 2019) and gibberellin (*MtCPS1*, *MtGA2ox10*, *MtGA3ox1*, and *MtDELLA2*) (Fonouni-Farde et al., 2016; Kim et al., 2019) biosynthesis and signaling genes. In addition, the expression of genes related to the jasmonic acid (*MtLOX6* [Gao et al., 2007] and *MtJAZ3* [Ge et al., 2016]), auxin (*MtARF10*) (Shen et al., 2015), abscisic acid (*MtABI5*) (Verdier et al., 2013), strigolactone (*MtD27*, *MtMAX1a*)

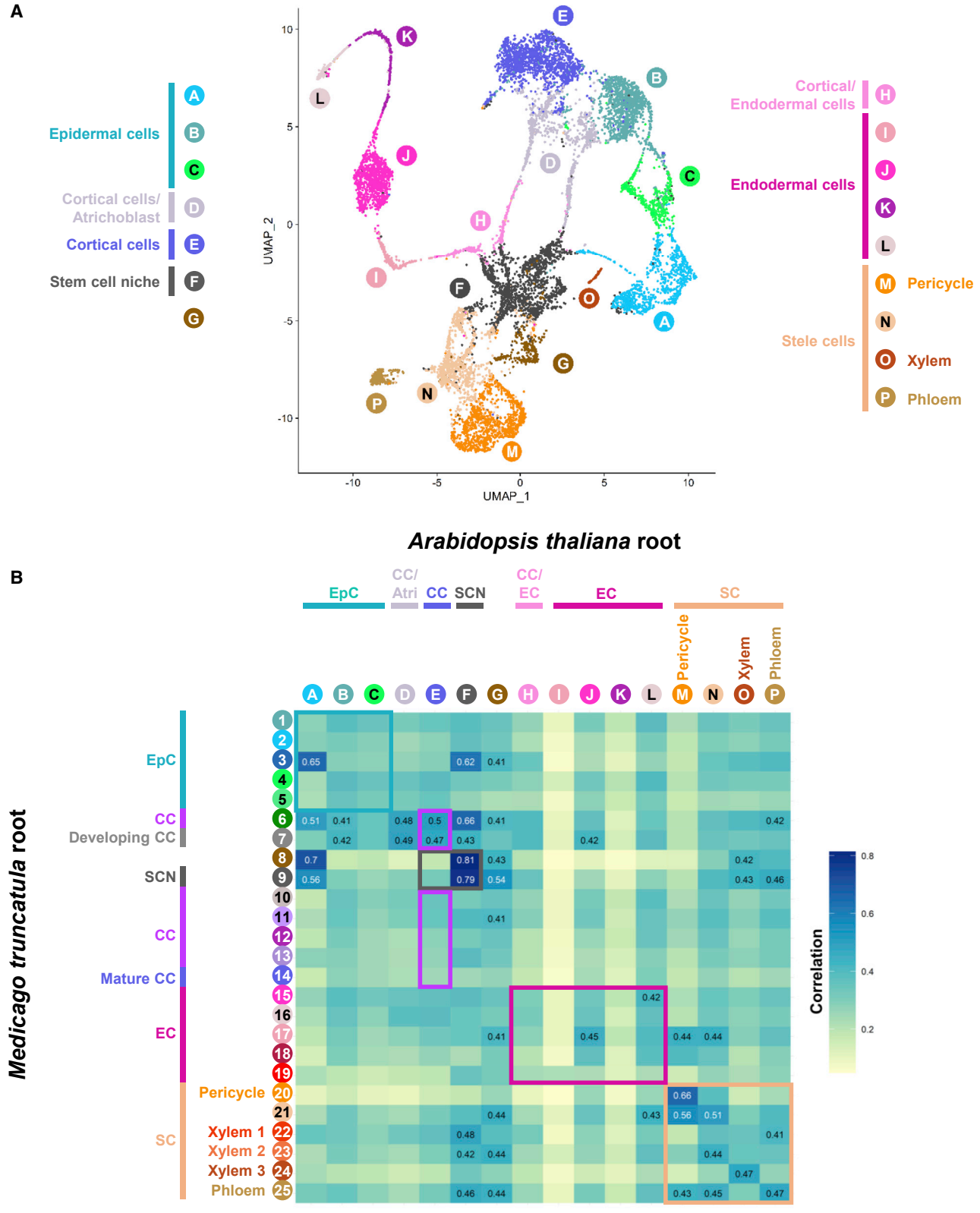

Figure 3. Comparative transcriptomic analysis of the *M. truncatula* and *A. thaliana* root cell clusters.
(A) Functional annotation of Arabidopsis root nuclei clusters based on the expression profile of cell-type marker genes defined from (Farmer et al., 2021).
(B) Pairwise correlations of Arabidopsis (*x* axis) and Medicago (*y* axis) root cell clusters. Only correlation numbers greater than 0.4 (black numbers) or 0.5 (white numbers) are shown in the heatmap. CC, cortical cells; EC, endodermal cells; EpC, epidermal cells; SC, stele cells; SCN, stem cell niche.

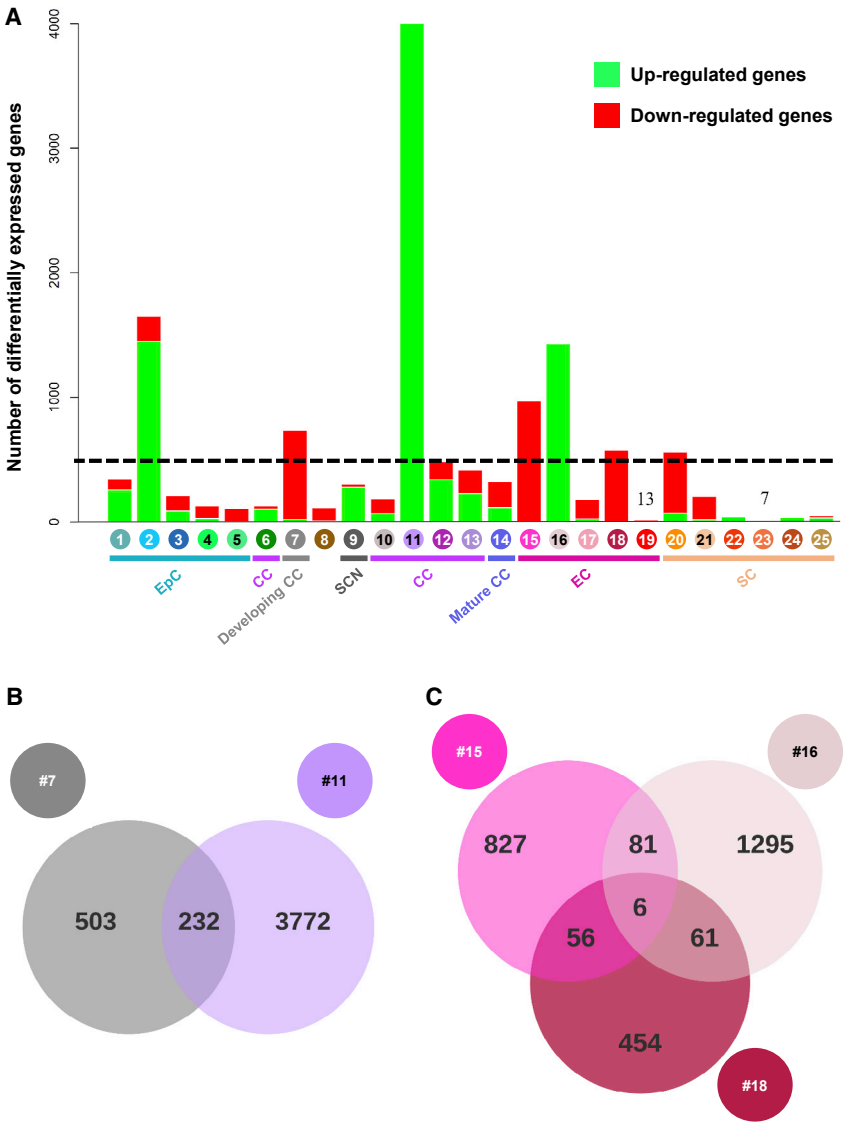

Figure 4. Differential expression of the *M. truncatula* genes in response to *E. meliloti* inoculation across the 25 root cell clusters.

(A) The transcriptional response of Medicago root cells to *E. meliloti* inoculation differs between cell-type clusters. The number of up- and down-regulated genes are highlighted in green and red bars, respectively. The dashed bar reflects the 500 DEGs thresholds.

(B and C) Comparison of the number of DEGs between the cortical cell clusters #7 and #11 **(B)** and between the endodermal cell clusters #15, #16, and #18 **(C)**. CC, cortical cells; EC, endodermal cells; EpC, epidermal cells; SC, stele cells; SCN, stem cell niche.

(Liu et al., 2011; Müller et al., 2019), ethylene (*MtETR4)* (Tan et al., 2019), and brassinosteroid (*MtBAK1*) (Tavormina et al., 2015) pathways were also upregulated upon rhizobium inoculation in cluster #2. Conversely, the expression of several genes encoding signaling peptides was repressed by rhizobium in cluster #2, such as *MtPIP1*, *MtIDA20*, *MtIDA31*, and *MtIDA35* (Inflorescence Deficient in Abscission) (de Bang et al., 2017) (Supplemental Tables 8 and 9, Figure 5). To further estimate the relevance of the trichoblast DEGs identified, we conducted a comparative analysis with the list of 267 DEGs previously reported in the Medicago root hair cells in response to rhizobium inoculation (Breakspear et al., 2014). We found that 99 of these genes (37%) were differentially expressed in the sNucRNA-seq dataset and, among them, 68 genes (69%) were significantly differentially expressed in at least one of the epidermal clusters #1, #2, or #3 (Supplemental Figure 5). Considering the difference in sensitivity between the technologies used, these results overall support the identification of genes differentially expressed in Medicago trichoblasts in response to rhizobia inoculation.

The cortical cell cluster #7 DEGs are all repressed upon rhizobium inoculation, including one gene, *MtCASTOR*, homologous to an *L. japonicus* nodulation gene (Charpentier et al., 2008), several cytokinin-related genes (two *LOG-like* genes and two *RRA* signaling genes, *MtRRA4* and *MtRRA9*), the gibberellin signaling gene *MtDELLA1*, and the abscisic acid signaling gene *MtABI5* (Supplemental Tables 8 and 9, Figure 5). Conversely, the cortical cell cluster #11 DEGs are all upregulated and include several genes controlling the rhizobia-infection process (*MtRbohA* [Marino et al., 2011], *MtRbohB*, and *MtLIN*), NF signaling (*MtPUB2*, *MtDMI1*, *MtDMI3*, and *MtERN2*), and nodule development (*MtSHR1*, *MtKNOX4*, and *MtKNOX9* [Di Giacomo et al., 2017], *MtNOOT1* and *MtCCS52a* [Cebolla et al., 1999]) and function (*MtNAC969*) (de Zélicourt et al., 2012)] (Supplemental Tables 8 and 9, Figure 5). In addition, hormonal genes related to cytokinin (*MtCHK1/MtCRE1* [Gonzalez-Rizzo et al., 2006], *MtHPT3*, *MtRRB5*, *MtRRB8*, and *MtRRA5*), auxin (*MtARF10*, *MtARF13*, and *MtARF24*), gibberellin (*MtDELLA2*), ethylene (*MtETR1*, *MtEIN3-like*), jasmonic acid (*MtLOX3* and *MtLOX6*), and strigolactone (*MtMAX2b*), were also upregulated upon rhizobium inoculation in cluster #11. Finally, two nitrate signaling-related TFs were upregulated (*MtNLP1* and *MtNLP4*) (Luo et al., 2021) as well as a specific signaling peptide (*MtRTF/DVL11*), in agreement with the symbiotic function previously reported for *MtDVL1* (Combier et al., 2008) (Supplemental Tables 8 and 9, Figure 5). Of note, despite the opposite transcriptional responses between clusters #7 and #11 to rhizobial inoculation, 232 genes out of the 736 DEGs in cluster #7 (31.5%) were shared as significantly differentially expressed with cluster #11 (Figure 4B). This indicates that an unexpectedly high number of genes show opposite transcriptional regulation in response to rhizobium within different cortical cell clusters. This exemplifies that reaching a cell type-specific level allows identifying that strong up- or downregulations can occur simultaneously in different clusters at the same 48 h after rhizobium inoculation time-point,

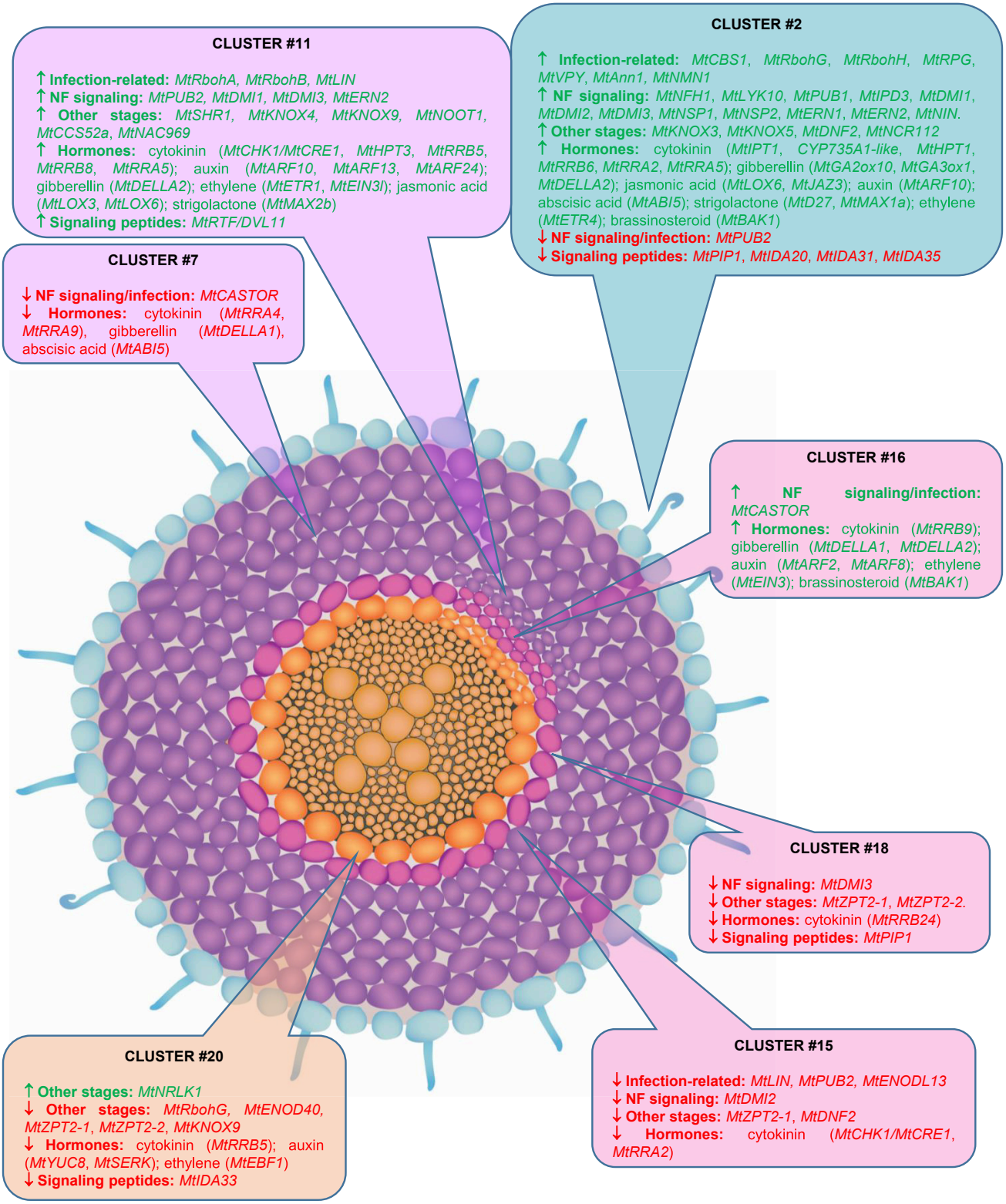

Figure 5. Summary of the *M. truncatula* root cell type-specific transcriptional response to rhizobial inoculation.
Selected genes previously known as related to nodulation and hormonal pathways and identified as differentially expressed in the clusters showing more than 500 DEGs are listed. Besides the expected induced expression pattern of numerous nodulation-related genes such as in the root hair cells cluster #2, more unexpected expression profiles were also highlighted notably for some late nodulation genes, and for repressed early nodulation and hormone-related genes in cortical and endodermal clusters #7 and #15–#18. Genes are listed in the following categories: rhizobial infection-related, NF signaling, other nodulation stages, hormones, and signaling peptides. Upward arrows indicate gene inductions by rhizobia, and downward arrows, repressions.

which would be thus likely missed if whole roots would be used. In addition, the differential transcriptional responses observed between cortical cell clusters for several hormonal pathways and root/nodule developmental genes upon rhizobial inoculation might mark cells that are activated for nodule organogenesis from those that are not, and may relate to the different layers of cortex (i.e., inner vs. outer), or correspond with cortical cells opposite to proto-phloem versus proto-xylem poles where nodule organogenesis is differentially initiated (Heidstra et al., 1997).

The endodermal clusters #15, #16, and #18, showing more than 500 DEGs, once more comprise either only downregulated genes (#15 and #18), or upregulated genes for cluster #16 (Figure 4A; Supplemental Table 7). In contrast with the cortical cell clusters, these endodermal clusters shared a limited number of DEGs (Figure 4C). Surprisingly, among clusters #15 and #18 downregulated genes, many early nodulation genes were observed, including for cluster #15 the infection-related genes *MtLIN*, *MtPUB2*, *MtENODL13*, the NF signaling-related gene *MtDMI2*, and the cytokinin signaling genes *MtCHK1/MtCRE1* and *MtRRA2*, as well as the late nodulation genes *MtZPT2-1* (Frugier et al., 2000) and *MtDNF2*; and for cluster #18, the NF signaling gene *MtDMI3*, the cytokinin signaling gene *MtRRB24*, the late nodulation genes *MtZPT2-1* and *MtZPT2-2*, and a signaling peptide, *MtPIP1* (Supplemental Tables 8 and 9, Figure 5). Concerning endodermis cluster #16 upregulated genes, the symbiotic-related gene *MtCASTOR* was retrieved, as well as several hormone-related genes including *MtARF2* and *MtARF8* (auxin), *MtDELLA1* and *MtDELLA2* (gibberellin), *MtRRB9* (cytokinin), *MtEIN3* (ethylene), and the co-receptor *MtBAK1*. In addition, the expression of the nitrate signaling-related *MtNLP1* gene was induced (Supplemental Tables 8 and 9, Figure 5).

Finally, in the pericycle (cluster #20), whereas the rhizobium-induced genes do not include any previously studied early nodulation genes, the *MtNRLK1* receptor-like kinase gene (Laffont et al., 2018) was retrieved as slightly induced in response to rhizobia. The *MtRbohG*, *MtENOD40*, *MtZPT2-1*, and *MtZPT2-2* nodulation genes were unexpectedly repressed by rhizobium, as well as the *MtKNOX9* developmental gene. Regarding hormone-related genes, the cytokinin *MtRRB5*, the auxin *MtYUC8*, and the ethylene *MtEBF1* gene, as well as the *MtIDA33* signaling peptide and the *MtSERK* co-receptor, were also repressed (Supplemental Tables 8 and 9, Figure 5).

Taken together, our unique dataset allowed a refined expression pattern analysis, which revealed unexpected cell-type specificity/enrichment for some of the already well-known early nodulation genes (e.g., a differential expression across cortical cell clusters and repression in endodermal cell clusters) or for the *MtCASTOR* gene which currently has no symbiotic function reported in *M.truncatula* unlike its homolog from *L. japonicus* (Venkateshwaran et al., 2012). In addition, some nodulation genes that were previously linked to later symbiotic stages (e.g., *MtNCR112*, *MtZPT2-1*, *MtZPT2-2*, *MtDNF2*, and *MtNAC969*) also showed a differential expression in response to rhizobium in specific root cell-type clusters. Surprisingly, a few anticipated early nodulation genes were missing from the DEG dataset (e.g., *MtLIN*, *MtNF-YA1*, and *MtNPL*), but a manual inspection of their expression profiles revealed differential regulations by rhizobia that were below the statistical threshold used. This indicates that our statistical analysis is conservative, allowing providing a robust dataset of DEGs, but also likely missing other genes of interest. More refined statistical analyses could be, however, performed in the future on this dataset, focusing only on a subset of specific clusters to extract such additional information that is currently lost because of the high variance between all nuclei analyzed.

Cell type-specific expression of nodulation and cytokinin-signaling related genes

As many nodulation-related genes can be already expressed in cells before bacterial inoculation, we additionally conducted a comprehensive analysis of their expression patterns independent of their response to rhizobial inoculation, focusing notably on genes showing cell type-enriched or -specific patterns that were not previously identified as DEGs (see above). Epidermal cells (#1–#5) most specifically expressed the *MtROP5* (Riely et al., 2011), *MtLIN*, and *MtPT5* (Wang et al., 2022) genes associated with rhizobial infections (clusters #2 and #3) (Damiani et al., 2016); *MtNFP*, *MtLYK3* (Smit et al., 2007), *MtLYK6*, *MtCNGC15c* (Charpentier et al., 2016), and *MtNF-YA1* genes, related to NF signaling (clusters #2 and #3); *MtCHIT5a* that is linked to NF degradation (clusters #4 and #5) (Tian et al., 2013), as well as genes related to late nodulation stages, namely *MtRab7A1* (Limpens et al., 2009), *MtSYP132* (Pan et al., 2016), *MtVPE* and *MtSPK1* (Andrio et al., 2013), *MtZIP6* (Abreu et al., 2017) (clusters #2 and #3), *MtDNF2* (cluster #4), *MtDGD1* (Si et al., 2019) (clusters #4 and #5), and *MtNAC969* (cluster #5); and *MtNLP1*, a gene linked to nitrate signaling (clusters #2 and #3) (Figure 6A).

In contrast, only a small number of previously characterized nodulation-related genes were specifically expressed/enriched in the non-annotated cluster #8, in the stem cell niche cluster #9, and in the cortical clusters #6, #7, and #10–#14 (i.e., *MtCHK1/CRE1*, a cytokinin receptor required for nodule organogenesis in cluster #7; *MtLATD/NIP*, an abscisic acid transporter linked to early nodulation in cluster #8 [Bagchi et al., 2012]; *MtBRI1*, a brassinosteroid receptor linked to nodulation [Cheng et al., 2017,] and *MtPIN2*, an auxin efflux carrier linked to nodule organogenesis in cluster #9 [Huo et al., 2006]; and *MtGlb1-1*, a gene involved in later nodulation stages in cluster #11 [Berger et al., 2020]) (Figure 6B).

In the endodermis (#15–#19), we identified several nodulation-related genes specifically expressed in one or several clusters (i.e., *MtKNOX5* [cluster #16], *MtRbohG*, *MtZPT2-1*, and *MtCDPK1* [cluster #18, as well as in the cortical cell cluster #14] [Ivashuta et al., 2005]), *MtCDPK3* (clusters #18 and #19), *MtKNOX3* (clusters #16 and #19), *MtANN1* (clusters #15 and #19), *MtDMI3* (cluster #19 in addition to the epidermal cell clusters #1, #2, and #3), *MtSYT3* (Gavrin et al., 2017), *MtTOP6A* (an ortholog to *LjSUNERGOS1* [Yoon et al., 2014]), and *MtMAPK6* (cluster #19[Chen et al., 2017]) (Figure 6C).

In the stele (#20–#25), a *LjTRICOT-like* gene (Suzaki et al., 2013), *MtMATE69* (Wang et al., 2017), and *MtTML2* (Gautrat et al., 2019)

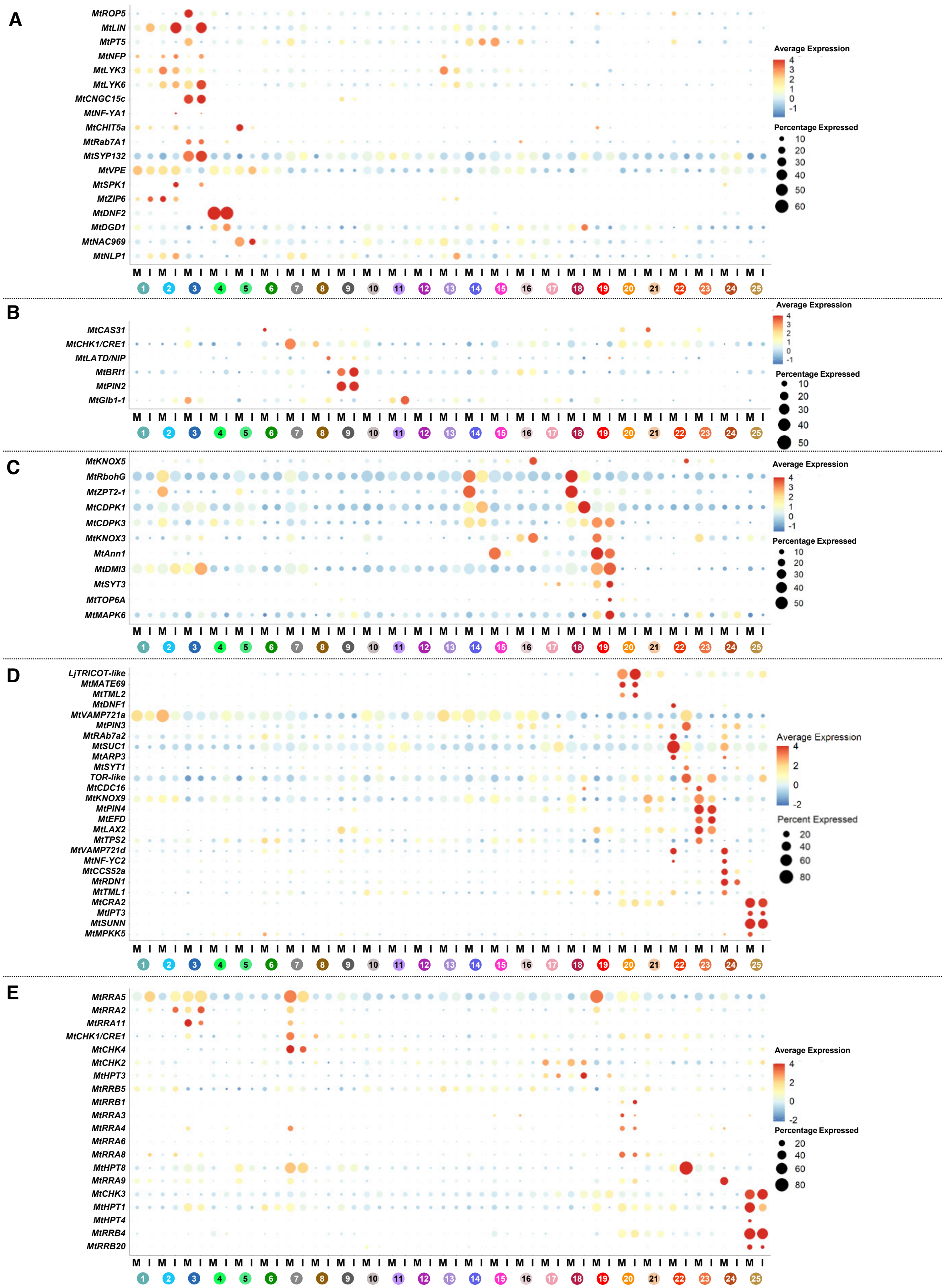

Figure 6. Cell-type enrichment of known *M. truncatula* nodulation and cytokinin signaling genes.
(A–E) Normalized expression levels of Medicago nodulation-related genes specifically expressed/enriched in the epidermal **(A)**, cortical **(B)**, endodermal **(C)**, and steles cells **(D)**, as well as of Medicago cytokinin signaling-related genes **(E)**. The 25 Medicago root clusters identified are shown on the *x* axis. The percentage of nuclei expressing the gene of interest (circle size), and the mean expression (circle color) of genes, are shown for each sub-panel. I, rhizobia-inoculated condition; M, mock-inoculated condition.

were specifically expressed in cluster #20 (pericycle cells), while *MtDNF1* (Van de Velde et al., 2010; Wang et al., 2010), *MtVAMP721a* (Sinharoy et al., 2013), *MtPIN3* (Huo et al., 2006), *MtRAb7a2* (Limpens et al., 2009), *MtSUC1* (Hohnjec et al., 2003), *MtARP3* (Gavrin et al., 2015), *MtSYT1* (Gavrin et al., 2017), TOR-like, *MtCDC16* (Kuppusamy et al., 2009), *MtKNOX9* and *MtPIN4* (Huo et al., 2006), *MtEFD* (Vernié et al., 2008), *MtLAX2* (Roy et al., 2017), *MtTPS2* and *MtVAMP721d* (Ivanov et al., 2012), *MtNF-YC2* (Baudin et al., 2015), *MtCCS52a*, and *MtRDN1* (Schnabel et al., 2011) were enriched in at least one of the xylem clusters (i.e., #22–#24). Finally, in cluster #25 (phloem), we identified several genes associated with the systemic regulation of nodulation (Gautrat et al., 2021), namely, *MtCRA2* (Huault et al., 2014; Mohd-Radzman et al., 2016), *MtSUNN*, *MtTML1* (Gautrat et al., 2019), *MtIPT3*, and *MtMPKK5* (Figure 6D). These observations are well supported by previous studies reporting the cell-type specificity of these genes.

Considering the cytokinin signaling pathway which is key for early nodulation (Gamas et al., 2017), we found *MtRRA5* most expressed in epidermal clusters #1–#3, as well as in clusters #7 (cortex) and #19 (endodermis), *MtRRA2* in clusters #2 and #3 (epidermis/root hairs), *MtRRA11* in clusters #3 (epidermis) and #7 (cortex), *MtCHK1/CRE1*, *MtCHK4*, *MtHPT8*, and *MtRRA4* in cluster #7 (cortex), *MtCHK2* and *MtHPT3* in clusters #17 and #18 (endodermis), *MtRRB5* in cluster #18 (endodermis), *MtRRB1*, *MtRRA3*, *MtRRA4*, *MtRRA6* and *MtRRA8* in cluster #20 (pericycle), *MtHPT8* and *MtRRA9* in clusters #22, #23, and #24 (xylem), and *MtCHK3*, *MtHPT1*, *MtHPT4*, *MtRRB4*, and *MtRRB20* in cluster #25 (phloem) (Figure 6E).

These results overall support that many early nodulation genes, including those involved in cytokinin signaling, have a cell-type specific/enriched expression pattern, indicating a coordinated activity between cell types to successfully promote nodule initiation. Interestingly, the co-regulation in a specific cluster of different genes belonging to a large family, or even to the same functional pathway, combined with phylogenetic analyses, now provides critical information to develop more efficient functional analyses to overcome functional redundancy. As an example, the *RRB* family related to cytokinin signaling contains 12 genes for which expression was detected in at least one cluster of the UMAP. Noteworthy, *MtRRB4* and *MtRRB20* have overlapping expression patterns in the phloem (cluster #25), suggesting a likely functional redundancy, also knowing their close phylogenetic relationship in the same clade (Tan et al., 2019). When combining this information with the expression pattern of genes from other cytokinin signaling families, a specific cytokinin signaling pathway preferentially acting in the phloem cells can now be identified, involving the MtCHK3 receptor, the MtHPT1 and MtHPT4 phosphotransfer proteins, and the MtRRB4 and MtRRB20 TFs. Similarly, when considering systemic pathways regulating nodulation (Gautrat et al., 2021), our analysis strikingly demonstrates that most known genes (i.e., *MtCRA2*, *MtSUNN*, *MtIPT3*, and *MtTML1*) are specifically expressed, and even induced by rhizobium in phloem cells (cluster #25). Importantly, getting access to such very detailed and clearcut spatial expression information allows generating innovative working hypotheses to be further tested functionally.

Root cell type-specific versus shared functional pathways enriched in response to a short-term rhizobium inoculation

To reveal new biological functions potentially controlling the response of Medicago root cell types to *E. meliloti*, we performed a gene ontology analysis using the Mapman software (Schwacke et al., 2019; Tellstrom et al., 2007) on the DEGs from clusters #2, #7, #11, #15, #16, #18, and #20 containing more than 500 DEGs (Figure 4A). The full list of enriched functional pathways is shown in Supplemental Table 10 and Supplemental Figure 6.

In cluster #2, functional pathways corresponding with changes in cellular organization, including modification of the cell wall (pectin esterases) and vesicle transport, were enriched for genes upregulated in response to bacterial inoculation (Wilcoxon rank-sum test, $p < 0.05$). This likely reflects the curling of root hairs associated with rhizobial infections. Among metabolic pathways, the flavonoid metabolism was enriched, notably the biosynthesis of dihydroflavonols, as well as the cytokinin and gibberellin biosynthesis pathways. This result strikingly fits with knowledge gained during the last decades where these three plant signaling pathways were shown as crucial for the regulation of early stages of rhizobial infections in the Medicago root epidermis (Gonzalez-Rizzo et al., 2006; Plet et al., 2011; Fonouni-Farde et al., 2016, 2017; Roy et al., 2019). In addition, both lysine motif and leucine-rich repeats receptor kinases were enriched in this trichoblast cluster #2 in response to rhizobium inoculation, which includes already known receptors required for rhizobial recognition and infection, as well as the phosphinositide metabolism and PHD finger or GRAS TFs, the latter family including also already known early nodulation genes. Concerning genes downregulated by rhizobia, the brassinosteroid and ethylene pathways were enriched, the latter hormone being previously extensively characterized as an inhibitor of rhizobial infections, notably in Medicago (Penmetsa et al., 2008).

Cortical cell clusters #7 downregulated DEGs showed enrichment for cell wall modifications and lipid metabolism, several hormonal pathways namely abscisic acid metabolism, ethylene signaling, as well as AP2/EREBP and Trihelix TF families; and cluster #11 upregulated DEGs for biotic stress responses, lipid, terpenoid, phenylpropanoid, and glucosinolate metabolic functions, as well as C2H2 zinc finger, CCAAT box binding factors, G2-like (GARP), and MYB-related TF families, the protein targeting secretory and protein degradation pathways (subtilases and autophagy), and cytoskeleton reorganization.

Endodermal cells clusters #15 and #18 (downregulated genes) were enriched for cell wall degradation and lipid metabolism functions, as well as ethylene and jasmonate metabolism, GRAS TF families, leucine-rich repeat receptor kinases, and protein degradation via ubiquitination. Regarding cluster #16 (upregulated genes), the biotic stress response and glucosinolate degradation functions were enriched, as well as the jasmonate hormone and the ARR TF family related to cytokinins, cell division and cell cycle, and sugar transport.

Finally, in pericycle cells (cluster #20), rhizobium downregulated genes were once more enriched for ethylene signaling pathway genes and AP2/EREBP TFs, as previously observed for the root hair cluster #2, the cortex cluster #7, and the endodermal clusters #15 and #18, highlighting one of the few shared biological responses across different cell types.

Overall, as previously noticed for the analysis of known nodulation-related genes, the novel cell-type specific information gained allows for generating new hypotheses, such as the existence of a tight interaction in inner root tissues of symbiotic responses with defense pathways through the modulation of specific specialized metabolite production. It also highlights specific hormonal pathways and TF families for which functional studies remain still limited, or even lacking, and that could thus be targeted in the future in relation to cell-type specific phenotypes (e.g., rhizobial infections or nodule organogenesis).

Plant root development requires tightly coordinated regulation of transcriptomic programs. We and others revealed root transcriptomic profiles at a single-cell level notably in the model plant *A. thaliana* (Denyer et al., 2019; Jean-Baptiste et al., 2019; Ryu et al., 2019; Shulse et al., 2019; Zhang et al., 2019; Farmer et al., 2021). In this study, we provide a comprehensive annotation of the Medicago root cell types according to their transcriptomic profiles, as well as an analysis of the transcriptomic response of Medicago root cells to rhizobial infection. Our study largely confirmed knowledge gained during the last decades in legume nodulation (i.e., the regulation of the expression of nodulation-related and hormonal genes known to regulate rhizobial infection and/or nodule organogenesis), but also nicely illustrates the gain of knowledge obtained using such single nuclei transcriptomic approaches to better understand the cell type specifically restricted responses of plants to microbial infection. The robust and high-quality dataset generated is also a resource to enable the discovery of new genes of interest not previously highlighted by bulk transcriptomic analyses. In particular, accessing cell-type information allows for generating more precise hypotheses regarding the symbiotic processes potentially affected by these novel candidate DEGs, and thus facilitates planning more appropriately experimental designs, notably by using tissue-specific promoters for which single-cell datasets are a key resource, and for performing refined focused phenotyping of rhizobial infections versus nodule organogenesis. The application of single-cell -omics technologies to other symbiotic and pathogenic plant-microbe interactions would help better understand the intimate complexity of the relationships between plants and microbes.

METHODS

Plant materials, root nucleus isolation, library preparation, and sequencing

Medicago seedlings were sterilized as described in Pingault et al. (2018). Eight seeds were then placed on agar B&D medium (Broughton and Dilworth, 1971) without nitrogen, and placed in a growth chamber in the dark for 4 days (26°C for 16 h and 20°C for 8 h). On the fourth day, 4 mL *E. meliloti* suspension (OD_{600nm} = 0.1), or water for the mock-inoculated samples, were applied to the seedlings' roots. The plates were placed back into the growth chamber for 48 h in the dark. On the sixth day, a subset of the *E. meliloti*-inoculated plants was transferred in vermiculite:perlite (3:1) and grown in the growth chamber (16 h daylight) for 3 weeks to confirm rhizobial infection and the formation of nodules. The remaining roots were used to collect the nuclei as described in Thibivilliers et al. (2020). The root samples used for these experiments were around 3–4 cm long, starting from the tip and ending in the zone where root hairs are fully differentiated, thus including the zone susceptible to rhizobial infection. Briefly, roots were then chopped and passed through a 30-μm cell strainer. The filtered nuclei were purified by cell sorting using FACSAria II cell sorter (BD Biosciences). An average of 80–100,000 nuclei were collected for each sample, centrifuged, and re-suspended in phosphate buffered saline-bovine serum albumin 0.5% RNA inhibitor solution. The six sNucRNA-seq libraries (i.e., three *E. meliloti*- and three mock-inoculated root libraries) were constructed following the Chromium Single Cell 3′ Library & Gel Bead Kit v3.1 protocol (10× Genomics). The sequencing of single-indexed paired-end libraries was performed on an Illumina NovaSeq 6000 platform according to the 10× Genomics recommendations.

Pre-processing of raw data, integration, clustering, and annotation

The six Medicago sNucRNA-seq libraries were preprocessed individually using the 10× Genomics Cell Ranger software v6.1.1.0, and then aligned against the latest version of the *Medicago truncatula* reference genome and genome annotation (https://medicago.toulouse.inra.fr/MtrunA17r5.0-ANR/) (Pecrix et al., 2018). Upon removal of background contamination using the SoupX software (Young and Behjati, 2020), filtration of doublets using the DoubletDetection prediction method (Adam Gayoso, 2022), and applying a statistical threshold on the data distribution (i.e., an interval of confidence of 95% to remove outliers) (see Supplemental Figure 1 to access the parameters for each sNucRNA-seq library), the normalization of individual sNucRNA-seq datasets and their respective integration to generate UMAPs was performed using Seurat V4 (Hao et al., 2021), selecting the top 2,000 variable genes for feature selection. Integration anchors were defined for the combined set of six sNucRNA-seq datasets based on the first 20 dimensions of the canonical correlation analysis method. After integration, the dimensionality reduction was performed with the first 40 principal components to generate the UMAP projection. Besides, the clustering was generated with the method FindClusters from Seurat with a resolution of 0.6. For downstream analyses, the expression values of each gene were calculated for each cluster using the AverageExpression function from Seurat.

For the annotation of cell types, the cluster-specific genes were identified with the FindAllMarkers function in Seurat. In addition, the expression patterns of known cell type-specific gene markers from *M.truncatula* (Supplemental Table 2 and Medicago genes orthologous to *A. thaliana* root cell-type marker genes were further analyzed (Farmer et al., 2021) (Supplemental Table 4).

UMAP visualization

For visualization purposes, all sNucRNA-seq libraries were combined using the Cell Ranger aggr function from 10× Genomics to combine all counts in a single cloupe file, and to show the UMAP coordinates projections and cell cluster assignments obtained from the Seurat analysis. We use ShinyCell (available at https://github.com/SGDDNB/ShinyCell), a web application allowing the visualization of single-cell data, to allow direct inquiries of the Medicago root single-cell transcriptome atlas (available from the https://shinycell.legumeinfo.org/medtr.A17.gnm5.ann1_6.expr.Cervantes-Perez_Thibivilliers_2022/web interface).

Differential gene expression analysis

To identify DEGs, raw read counts were extracted to calculate a normalized average expression for each gene, in each cluster, and for each condition (Supplemental Table 9) before applying the DEsingle package (Miao et al., 2018) using a p value of less than 0.05 and FC of greater than 1.5 thresholds. This package allows the identification of DEGs between *E. meliloti*- and mock-inoculated nuclei in a raw read count matrix employing the zero-inflated negative binomial model (Wang et al., 2019).

Correlation analysis between plant root single nuclei transcriptomes

To support the functional annotation in the *M.truncatula* root clusters, we compared the transcriptomes of the different Medicago root clusters upon

extracting the pseudo-bulk expression of each gene among all clusters and then conducted Pearson's correlation analyses to reveal the most similar transcriptomes among all nuclei clusters.

To compare the transcriptome of Medicago and Arabidopsis root clusters, *A. thaliana* sNucRNA-seq datasets were obtained from previously published data (Farmer et al., 2021), based on the following SRA files: GSM4698755, GSM4698756, GSM4698757, GSM4698758, and GSM4698759. The five replicates were processed individually using the 10× Genomics Cell Ranger v6.1.1.0 pipeline, and then mapped against a reference genome constructed with TAIR10.26 genome and Araport11 annotations. The same parameters were then used for preprocessing the Arabidopsis datasets as previously used for the Medicago sNucRNA-seq datasets (see above). To correlate the *A. thaliana* and *M.truncatula* root sNuc transcriptomes, we extracted pseudo-bulk information for the one-to-one orthologs between the two plant species (CoGe; https://genomevolution.org/coge/) (Lyons et al., 2008; Lyons and Freeling, 2008) and conducted a Pearson's correlation analysis between the expression of these orthologous genes for each cell cluster.

Genes of interest and functional classification analyses

The Legoo knowledge base (https://lipm-browsers.toulouse.inra.fr/k/legoo/) was used to identify genes of interest (Carrère et al., 2019), as well as the Mapman software (https://mapman.gabipd.org/) for the analysis of gene functions (Thimm et al., 2004).

ACCESSION NUMBERS

Expression data are available at the Gene Expression Omnibus (GEO: GSE210881). The Medicago root single-cell transcriptome atlas can be accessed through https://shinycell.legumeinfo.org/medtr.A17.gnm5.ann1_6.expr.Cervantes-Perez_Thibivilliers_2022/.

SUPPLEMENTAL INFORMATION

Supplemental information is available at *Molecular Plant Online*.

FUNDING

Supported by grants to M.L. from the U.S. National Science Foundation (IOS #1854326 and 2127485), USDA-NIFA (#2022-67013-36144), by the Center for Plant Science Innovation, and by the Department of Agronomy and Horticulture at the University of Nebraska-Lincoln. Work in F.F. laboratory was supported by the "Ecole Universitaire de Recherche" Saclay Plant Sciences (EUR-SPS).

AUTHOR CONTRIBUTIONS

S.T. performed experiments. S.A.C.P., S.T., C.L., A.D.F., F.F., and M.L. carried out data analysis. M.L. coordinated the study. S.A.C.P., S.T., F.F., and M.L. drafted the manuscript. All authors contributed to the preparation of the manuscript.

ACKNOWLEDGMENTS

The authors acknowledge Lana Koepke Johnson from the Department of Agronomy and Horticulture at the University of Nebraska–Lincoln for her artistic work to create Figure 5. We also acknowledge Dirk Anderson, manager of the Flow Cytometry Core Facility, the Single Cell Genomics Core Facility, and the Nebraska Center for Biotechnology at the University of Nebraska–Lincoln, for providing support in the sorting of the isolated nuclei and for their processing to generate sNucRNA-seq libraries. No conflict of interest declared.

Received: August 10, 2022
Revised: October 5, 2022
Accepted: October 27, 2022
Published: November 1, 2022; corrected online: January 6, 2023

REFERENCES

Abreu, I., Saéz, Á., Castro-Rodríguez, R., Escudero, V., Rodríguez-Haas, B., Senovilla, M., Larue, C., Grolimund, D., Tejada-Jiménez, M., Imperial, J., et al. (2017). *Medicago truncatula* Zinc-Iron Permease6 provides zinc to rhizobia-infected nodule cells. Plant Cell Environ. **40**:2706–2719. https://doi.org/10.1111/pce.13035.

Adam Gayoso, J.S. (2022). JonathanShor/DoubletDetection: doubletdetection v4.2 (v4.). Zenodo. https://doi.org/10.5281/zenodo.6349517.

Alunni, B., Kevei, Z., Redondo-Nieto, M., Kondorosi, A., Mergaert, P., and Kondorosi, E. (2007). Genomic organization and evolutionary insights on *GRP* and *NCR* genes, two large nodule-specific gene families in *Medicago truncatula*. Mol. Plant Microbe Interact. **20**:1138–1148. https://doi.org/10.1094/mpmi-20-9-1138.

Andriankaja, A., Boisson-Dernier, A., Frances, L., Sauviac, L., Jauneau, A., Barker, D.G., and de Carvalho-Niebel, F. (2007). AP2-ERF transcription factors mediate Nod factor dependent MtENOD11 activation in root hairs via a novel cis-regulatory motif. Plant Cell **19**:2866–2885. https://doi.org/10.1105/tpc.107.052944.

Andrio, E., Marino, D., Marmeys, A., de Segonzac, M.D., Damiani, I., Genre, A., Huguet, S., Frendo, P., Puppo, A., and Pauly, N. (2013). Hydrogen peroxide-regulated genes in the *Medicago truncatula-Sinorhizobium meliloti* symbiosis. New Phytol. **198**:179–189. https://doi.org/10.1111/nph.12120.

Ané, J.M., Kiss, G.B., Riely, B.K., Penmetsa, R.V., Oldroyd, G.E., Ayax, C., Lévy, J., Debellé, F., Baek, J.M., Kalo, P., et al. (2004). Medicago truncatula *DMI1* required for bacterial and fungal symbioses in legumes. Science **303**:1364–1367. https://doi.org/10.1126/science.1092986.

Arrighi, J.-F., Godfroy, O., Billy, F.d., Saurat, O., Jauneau, A., and Gough, C. (2008). The *RPG* gene of *Medicago truncatula* controls Rhizobium-directed polar growth during infection. Proc. Natl. Acad. Sci. USA **105**:9817–9822. https://doi.org/10.1073/pnas.0710273105.

Azarakhsh, M., Lebedeva, M.A., and Lutova, L.A. (2018). Identification and expression analysis of *Medicago truncatula* isopentenyl transferase genes (IPTs) involved in local and systemic control of nodulation. Front. Plant Sci. **9**:304. https://doi.org/10.3389/fpls.2018.00304.

Bagchi, R., Salehin, M., Adeyemo, O.S., Salazar, C., Shulaev, V., Sherrier, D.J., and Dickstein, R. (2012). Functional assessment of the *Medicago truncatula* NIP/LATD protein demonstrates that it is a high-affinity nitrate transporter. Plant Physiol. **160**:906–916. https://doi.org/10.1104/pp.112.196444.

Baudin, M., Laloum, T., Lepage, A., Rípodas, C., Ariel, F., Frances, L., Crespi, M., Gamas, P., Blanco, F.A., Zanetti, M.E., et al. (2015). A phylogenetically conserved group of nuclear factor-Y transcription factors interact to control nodulation in legumes. Plant Physiol. **169**:2761–2773. https://doi.org/10.1104/pp.15.01144.

Berger, A., Guinand, S., Boscari, A., Puppo, A., and Brouquisse, R. (2020). *Medicago truncatula Phytoglobin 1.1* controls symbiotic nodulation and nitrogen fixation via the regulation of nitric oxide concentration. New Phytol. **227**:84–98. https://doi.org/10.1111/nph.16462.

Bhuvaneswari, T.V., Bhagwat, A.A., and Bauer, W.D. (1981). Transient susceptibility of root cells in four common legumes to nodulation by rhizobia. Plant Physiol **68**:1144–1149.

Biala, W., Banasiak, J., Jarzyniak, K., Pawela, A., and Jasinski, M. (2017). *Medicago truncatula* ABCG10 is a transporter of 4-coumarate and liquiritigenin in the medicarpin biosynthetic pathway. J. Exp. Bot. **68**:3231–3241. https://doi.org/10.1093/jxb/erx059.

Birnbaum, K., Shasha, D.E., Wang, J.Y., Jung, J.W., Lambert, G.M., Galbraith, D.W., and Benfey, P.N. (2003). A gene expression map of the Arabidopsis root. Science **302**:1956–1960. https://doi.org/10.1126/science.1090022.

Böhme, K., Li, Y., Charlot, F., Grierson, C., Marrocco, K., Okada, K., Laloue, M., and Nogué, F. (2004). The Arabidopsis *COW1* gene encodes a phosphatidylinositol transfer protein essential for root hair tip growth. Plant J. **40**:686–698. https://doi.org/10.1111/j.1365-313X.2004.02245.x.

Boivin, S., Fonouni-Farde, C., and Frugier, F. (2016). How auxin and cytokinin phytohormones modulate root microbe interactions. Front. Plant Sci. **7**:1240. https://doi.org/10.3389/fpls.2016.01240.

Bourcy, M., Brocard, L., Pislariu, C.I., Cosson, V., Mergaert, P., Tadege, M., Mysore, K.S., Udvardi, M.K., Gourion, B., and Ratet, P. (2013). *Medicago truncatula* DNF2 is a PI-PLC-XD-containing protein required for bacteroid persistence and prevention of nodule early senescence and defense-like reactions. New Phytol. **197**:1250–1261. https://doi.org/10.1111/nph.12091.

Breakspear, A., Liu, C., Roy, S., Stacey, N., Rogers, C., Trick, M., Morieri, G., Mysore, K.S., Wen, J., Oldroyd, G.E.D., et al. (2014). The root hair "infectome" of *Medicago truncatula* uncovers changes in cell cycle genes and reveals a requirement for auxin signaling in rhizobial infection. Plant Cell **26**:4680–4701. https://doi.org/10.1105/tpc.114.133496.

Broughton, W.J., and Dilworth, M.J. (1971). Control of leghaemoglobin synthesis in snake beans. Biochem. J. **125**:1075–1080. https://doi.org/10.1042/bj1251075.

Cai, J., Zhang, L.-Y., Liu, W., Tian, Y., Xiong, J.-S., Wang, Y.-H., Li, R.-J., Li, H.-M., Wen, J., Mysore, K.S., et al. (2018). Role of the Nod factor hydrolase MtNFH1 in regulating Nod factor levels during rhizobial infection and in mature nodules of *Medicago truncatula*. Plant Cell **30**:397–414. https://doi.org/10.1105/tpc.17.00420.

Carrère, S., Verdenaud, M., Gough, C., Gouzy, J., and Gamas, P. (2019). LeGOO: an expertized knowledge database for the model legume *Medicago truncatula*. Plant Cell Physiol. **61**:203–211. https://doi.org/10.1093/pcp/pcz177.

Cebolla, A., María Vinardell, J., Kiss, E., Oláh, B., Roudier, F., Kondorosi, A., and Kondorosi, E. (1999). The mitotic inhibitor ccs52 is required for endoreduplication and ploidy-dependent cell enlargement in plants. EMBO J. **18**:4476–4484. https://doi.org/10.1093/emboj/18.16.4476.

Cerri, M.R., Frances, L., Kelner, A., Fournier, J., Middleton, P.H., Auriac, M.C., Mysore, K.S., Wen, J., Erard, M., Barker, D.G., et al. (2016). The symbiosis-related ERN transcription factors act in concert to coordinate rhizobial host root infection. Plant Physiol. **171**:1037–1054. https://doi.org/10.1104/pp.16.00230.

Charpentier, M., Bredemeier, R., Wanner, G., Takeda, N., Schleiff, E., and Parniske, M. (2008). Lotus japonicus CASTOR and POLLUX are ion channels essential for perinuclear calcium spiking in legume root endosymbiosis. Plant Cell **20**:3467–3479. https://doi.org/10.1105/tpc.108.063255.

Charpentier, M., Sun, J., Martins, T.V., Radhakrishnan, G.V., Findlay, K., Soumpourou, E., Thouin, J., Véry, A.-A., Sanders, D., Morris, R.J., et al. (2016). Nuclear-localized cyclic nucleotide-gated channels mediate symbiotic calcium oscillations. Science **352**:1102–1105. https://doi.org/10.1126/science.aae0109.

Chen, T., Zhou, B., Duan, L., Zhu, H., and Zhang, Z. (2017). *MtMAPKK4* is an essential gene for growth and reproduction of *Medicago truncatula*. Physiol. Plantarum **159**:492–503. https://doi.org/10.1111/ppl.12533.

Cheng, X., Gou, X., Yin, H., Mysore, K.S., Li, J., and Wen, J. (2017). Functional characterisation of brassinosteroid receptor MtBRI1 in *Medicago truncatula*. Sci. Rep. **7**:9327. https://doi.org/10.1038/s41598-017-09297-9.

Chiou, T.-J., Liu, H., and Harrison, M.J. (2001). The spatial expression patterns of a phosphate transporter (MtPT1) from *Medicago truncatula* indicate a role in phosphate transport at the root/soil interface. Plant J. **25**:281–293. https://doi.org/10.1046/j.1365-313x.2001.00963.x.

Combier, J.-P., Frugier, F., de Billy, F., Boualem, A., El-Yahyaoui, F., Moreau, S., Vernié, T., Ott, T., Gamas, P., Crespi, M., et al. (2006). MtHAP2-1 is a key transcriptional regulator of symbiotic nodule development regulated by microRNA169 in *Medicago truncatula*. Genes Dev. **20**:3084–3088. https://doi.org/10.1101/gad.402806.

Combier, J.P., Küster, H., Journet, E.P., Hohnjec, N., Gamas, P., and Niebel, A. (2008). Evidence for the involvement in nodulation of the two small putative regulatory peptide-encoding genes *MtRALFL1* and *MtDVL1*. Mol. Plant Microbe Interact. **21**:1118–1127. https://doi.org/10.1094/mpmi-21-8-1118.

Cvrčková, F., Bezvoda, R., and Zárský, V. (2010). Computational identification of root hair-specific genes in Arabidopsis. Plant Signal. Behav. **5**:1407–1418. https://doi.org/10.4161/psb.5.11.13358.

Damiani, I., Drain, A., Guichard, M., Balzergue, S., Boscari, A., Boyer, J.C., Brunaud, V., Cottaz, S., Rancurel, C., Da Rocha, M., et al. (2016). Nod factor effects on root hair-specific transcriptome of *Medicago truncatula*: focus on plasma membrane transport systems and reactive oxygen species networks. Front. Plant Sci. **7**:794. https://doi.org/10.3389/fpls.2016.00794.

de Bang, T.C., Lundquist, P.K., Dai, X., Boschiero, C., Zhuang, Z., Pant, P., Torres-Jerez, I., Roy, S., Nogales, J., Veerappan, V., et al. (2017). Genome-Wide identification of Medicago peptides involved in macronutrient responses and nodulation. Plant Physiol. **175**:1669–1689. https://doi.org/10.1104/pp.17.01096.

de Carvalho Niebel, F., Lescure, N., Cullimore, J.V., and Gamas, P. (1998). The *Medicago truncatula MtAnn1* gene encoding an annexin is induced by Nod factors and during the symbiotic interaction with rhizobium meliloti. Mol. Plant Microbe Interact. **11**:504–513. https://doi.org/10.1094/mpmi.1998.11.6.504.

de Zélicourt, A., Diet, A., Marion, J., Laffont, C., Ariel, F., Moison, M., Zahaf, O., Crespi, M., Gruber, V., and Frugier, F. (2012). Dual involvement of a *Medicago truncatula* NAC transcription factor in root abiotic stress response and symbiotic nodule senescence. Plant J. **70**:220–230. https://doi.org/10.1111/j.1365-313X.2011.04859.x.

Denyer, T., Ma, X., Klesen, S., Scacchi, E., Nieselt, K., and Timmermans, M.C.P. (2019). Spatiotemporal developmental trajectories in the Arabidopsis root revealed using high-throughput single-cell RNA sequencing. Dev. Cell **48**:840–852.e5. https://doi.org/10.1016/j.devcel.2019.02.022.

Di Giacomo, E., Laffont, C., Sciarra, F., Iannelli, M.A., Frugier, F., and Frugis, G. (2017). KNAT3/4/5-like class 2 KNOX transcription factors are involved in *Medicago truncatula* symbiotic nodule organ development. New Phytol. **213**:822–837. https://doi.org/10.1111/nph.14146.

Dolgikh, E.A., Kusakin, P.G., Kitaeva, A.B., Tsyganova, A.V., Kirienko, A.N., Leppyanen, I.V., Dolgikh, A.V., Ilina, E.L., Demchenko, K.N., Tikhonovich, I.A., et al. (2020). Mutational analysis indicates that abnormalities in rhizobial infection and subsequent plant cell and bacteroid differentiation in pea (*Pisum sativum*) nodules coincide with abnormal cytokinin responses and localization. Ann. Bot. **125**:905–923. https://doi.org/10.1093/aob/mcaa022.

Dong, W., Zhu, Y., Chang, H., Wang, C., Yang, J., Shi, J., Gao, J., Yang, W., Lan, L., Wang, Y., et al. (2021). An SHR-SCR module specifies legume cortical cell fate to enable nodulation. Nature **589**:586–590. https://doi.org/10.1038/s41586-020-3016-z.

Endre, G., Kereszt, A., Kevei, Z., Mihacea, S., Kaló, P., and Kiss, G.B. (2002). A receptor kinase gene regulating symbiotic nodule development. Nature **417**:962–966. https://doi.org/10.1038/nature00842.

Farmer, A., Thibivilliers, S., Ryu, K.H., Schiefelbein, J., and Libault, M. (2021). Single-nucleus RNA and ATAC sequencing reveals the impact

of chromatin accessibility on gene expression in Arabidopsis roots at the single-cell level. Mol. Plant **14**:372–383. https://doi.org/10.1016/j.molp.2021.01.001.

Fendrych, M., Van Hautegem, T., Van Durme, M., Olvera-Carrillo, Y., Huysmans, M., Karimi, M., Lippens, S., Guérin, C.J., Krebs, M., Schumacher, K., et al. (2014). Programmed cell death controlled by ANAC033/SOMBRERO determines root cap organ size in Arabidopsis. Curr. Biol. **24**:931–940. https://doi.org/10.1016/j.cub.2014.03.025.

Fonouni-Farde, C., Kisiala, A., Brault, M., Emery, R.J.N., Diet, A., and Frugier, F. (2017). DELLA1-Mediated gibberellin signaling regulates cytokinin-dependent symbiotic nodulation. Plant Physiol. **175**:1795–1806. https://doi.org/10.1104/pp.17.00919.

Fonouni-Farde, C., Tan, S., Baudin, M., Brault, M., Wen, J., Mysore, K.S., Niebel, A., Frugier, F., and Diet, A. (2016). DELLA-mediated gibberellin signalling regulates Nod factor signalling and rhizobial infection. Nat. Commun. **7**:12636. https://doi.org/10.1038/ncomms12636.

Franssen, H.J., Xiao, T.T., Kulikova, O., Wan, X., Bisseling, T., Scheres, B., and Heidstra, R. (2015). Root developmental programs shape the *Medicago truncatula* nodule meristem. Development **142**:2941–2950. https://doi.org/10.1242/dev.120774.

Frugier, F., Poirier, S., Satiat-Jeunemaitre, B., Kondorosi, A., and Crespi, M. (2000). A Krüppel-like zinc finger protein is involved in nitrogen-fixing root nodule organogenesis. Genes Dev. **14**:475–482.

Gamas, P., Brault, M., Jardinaud, M.F., and Frugier, F. (2017). Cytokinins in symbiotic nodulation: when, where, what for? Trends Plant Sci. **22**:792–802. https://doi.org/10.1016/j.tplants.2017.06.012.

Gao, L.L., Anderson, J.P., Klingler, J.P., Nair, R.M., Edwards, O.R., and Singh, K.B. (2007). Involvement of the octadecanoid pathway in bluegreen aphid resistance in *Medicago truncatula*. Mol. Plant Microbe Interact. **20**:82–93. https://doi.org/10.1094/mpmi-20-0082.

Gaude, N., Bortfeld, S., Duensing, N., Lohse, M., and Krajinski, F. (2012). Arbuscule-containing and non-colonized cortical cells of mycorrhizal roots undergo extensive and specific reprogramming during arbuscular mycorrhizal development. Plant J. **69**:510–528. https://doi.org/10.1111/j.1365-313X.2011.04810.x.

Gautrat, P., Laffont, C., Frugier, F., and Ruffel, S. (2021). Nitrogen systemic signaling: from symbiotic nodulation to root acquisition. Trends Plant Sci. **26**:392–406. https://doi.org/10.1016/j.tplants.2020.11.009.

Gautrat, P., Mortier, V., Laffont, C., De Keyser, A., Fromentin, J., Frugier, F., and Goormachtig, S. (2019). Unraveling new molecular players involved in the autoregulation of nodulation in *Medicago truncatula*. J. Exp. Bot. **70**:1407–1417. https://doi.org/10.1093/jxb/ery465.

Gavrin, A., Kulikova, O., Bisseling, T., and Fedorova, E.E. (2017). Interface symbiotic membrane formation in root nodules of *Medicago truncatula*: the role of synaptotagmins MtSyt1, MtSyt2 and MtSyt3. Front. Plant Sci. **8**. https://doi.org/10.3389/fpls.2017.00201.

Gavrin, A., Jansen, V., Ivanov, S., Bisseling, T., and Fedorova, E. (2015). ARP2/3-Mediated actin nucleation associated with symbiosome membrane is essential for the development of symbiosomes in infected cells of *Medicago truncatula* root nodules. Mol. Plant Microbe Interact. **28**:605–614. https://doi.org/10.1094/mpmi-12-14-0402-r.

Ge, L., Yu, J., Wang, H., Luth, D., Bai, G., Wang, K., and Chen, R. (2016). Increasing seed size and quality by manipulating BIG SEEDS1 in legume species. Proc. Natl. Acad. Sci. USA **113**:12414–12419. https://doi.org/10.1073/pnas.1611763113.

Gleason, C., Chaudhuri, S., Yang, T., Muñoz, A., Poovaiah, B.W., and Oldroyd, G.E. (2006). Nodulation independent of rhizobia induced by a calcium-activated kinase lacking autoinhibition. Nature **441**:1149–1152. https://doi.org/10.1038/nature04812.

Gonzalez-Rizzo, S., Crespi, M., and Frugier, F. (2006). The *Medicago truncatula* CRE1 cytokinin receptor regulates lateral root development and early symbiotic interaction with *Sinorhizobium meliloti*. Plant Cell **18**:2680–2693. https://doi.org/10.1105/tpc.106.043778.

Gough, C., Cottret, L., Lefebvre, B., and Bono, J.-J. (2018). Evolutionary history of plant LysM receptor proteins related to root endosymbiosis. Front. Plant Sci. **9**. https://doi.org/10.3389/fpls.2018.00923.

Haney, C.H., and Long, S.R. (2010). Plant flotillins are required for infection by nitrogen-fixing bacteria. Proc. Natl. Acad. Sci. USA **107**:478–483. https://doi.org/10.1073/pnas.0910081107.

Hao, Y., Hao, S., Andersen-Nissen, E., Mauck, W.M., Zheng, S., Butler, A., Lee, M.J., Wilk, A.J., Darby, C., Zager, M., et al. (2021). Integrated analysis of multimodal single-cell data. Cell **184**:3573–3587.e29. https://doi.org/10.1016/j.cell.2021.04.048.

Heidstra, R., Yang, W.C., Yalcin, Y., Peck, S., Emons, A.M., van Kammen, A., and Bisseling, T. (1997). Ethylene provides positional information on cortical cell division but is not involved in Nod factor-induced root hair tip growth in Rhizobium-legume interaction. Development (Cambridge, England) **124**:1781–1787. https://doi.org/10.1242/dev.124.9.1781.

Heo, J.-o., Blob, B., and Helariutta, Y. (2017). Differentiation of conductive cells: a matter of life and death. Curr. Opin. Plant Biol. **35**:23–29. https://doi.org/10.1016/j.pbi.2016.10.007.

Hohnjec, N., Perlick, A.M., Pühler, A., and Küster, H. (2003). The *Medicago truncatula* sucrose synthase gene *MtSucS1* is activated both in the infected region of root nodules and in the cortex of roots colonized by arbuscular mycorrhizal Fungi. Mol. Plant Microbe Interact. **16**:903–915. https://doi.org/10.1094/mpmi.2003.16.10.903.

Huault, E., Laffont, C., Wen, J., Mysore, K.S., Ratet, P., Duc, G., and Frugier, F. (2014). Local and systemic regulation of plant root system Architecture and symbiotic nodulation by a receptor-like kinase. PLoS Genet. **10**:e1004891. https://doi.org/10.1371/journal.pgen.1004891.

Huo, X., Schnabel, E., Hughes, K., and Frugoli, J. (2006). RNAi phenotypes and the localization of a protein::GUS Fusion imply a role for *Medicago truncatula PIN* genes in nodulation. J. Plant Growth Regul. **25**:156–165. https://doi.org/10.1007/s00344-005-0106-y.

Ivanov, S., Fedorova, E.E., Limpens, E., De Mita, S., Genre, A., Bonfante, P., and Bisseling, T. (2012). Rhizobium-legume symbiosis shares an exocytotic pathway required for arbuscule formation. Proc. Natl. Acad. Sci. USA **109**:8316–8321. https://doi.org/10.1073/pnas.1200407109.

Ivashuta, S., Liu, J., Liu, J., Lohar, D.P., Haridas, S., Bucciarelli, B., VandenBosch, K.A., Vance, C.P., Harrison, M.J., and Gantt, J.S. (2005). RNA interference identifies a calcium-dependent protein kinase involved in *Medicago truncatula* root development. Plant Cell **17**:2911–2921. https://doi.org/10.1105/tpc.105.035394.

Jardinaud, M.F., Boivin, S., Rodde, N., Catrice, O., Kisiala, A., Lepage, A., Moreau, S., Roux, B., Cottret, L., Sallet, E., et al. (2016). A laser dissection-RNAseq analysis highlights the activation of cytokinin pathways by Nod factors in the *Medicago truncatula* root epidermis. Plant Physiol. **171**:2256–2276. https://doi.org/10.1104/pp.16.00711.

Jean-Baptiste, K., McFaline-Figueroa, J.L., Alexandre, C.M., Dorrity, M.W., Saunders, L., Bubb, K.L., Trapnell, C., Fields, S., Queitsch, C., and Cuperus, J.T. (2019). Dynamics of gene expression in single root cells of *Arabidopsis thaliana*. Plant Cell **31**:993–1011. https://doi.org/10.1105/tpc.18.00785.

Kaló, P., Gleason, C., Edwards, A., Marsh, J., Mitra, R.M., Hirsch, S., Jakab, J., Sims, S., Long, S.R., Rogers, J., et al. (2005). Nodulation

signaling in legumes requires NSP2, a member of the GRAS family of transcriptional regulators. Science **308**:1786–1789. https://doi.org/10.1126/science.1110951.

Kassaw, T., Nowak, S., Schnabel, E., and Frugoli, J. (2017). ROOT DETERMINED NODULATION1 is required for *M. truncatula* CLE12, but not CLE13, peptide signaling through the SUNN receptor kinase. Plant Physiol. **174**:2445–2456. https://doi.org/10.1104/pp.17.00278.

Kim, G.B., Son, S.U., Yu, H.J., and Mun, J.H. (2019). MtGA2ox10 encoding C20-GA2-oxidase regulates rhizobial infection and nodule development in *Medicago truncatula*. Sci. Rep. **9**:5952. https://doi.org/10.1038/s41598-019-42407-3.

Kiss, E., Oláh, B.r., Kaló, P.t., Morales, M., Heckmann, A.B., Borbola, A., Lózsa, A., Kontár, K., Middleton, P., Downie, J.A., et al. (2009). LIN, a novel type of U-Box/WD40 protein, controls early infection by rhizobia in legumes. Plant Physiol. **151**:1239–1249. https://doi.org/10.1104/pp.109.143933.

Kumpf, R.P., and Nowack, M.K. (2015). The root cap: a short story of life and death. J. Exp. Bot. **66**:5651–5662. https://doi.org/10.1093/jxb/erv295.

Kuppusamy, K.T., Ivashuta, S., Bucciarelli, B., Vance, C.P., Gantt, J.S., and VandenBosch, K.A. (2009). Knockdown of *CELL DIVISION CYCLE16* reveals an inverse relationship between lateral root and nodule numbers and a link to auxin in *Medicago truncatula*. Plant Physiol. **151**:1155–1166. https://doi.org/10.1104/pp.109.143024.

Laffont, C., De Cuyper, C., Fromentin, J., Mortier, V., De Keyser, A., Verplancke, C., Holsters, M., Goormachtig, S., and Frugier, F. (2018). MtNRLK1, a CLAVATA1-like leucine-rich repeat receptor-like kinase upregulated during nodulation in *Medicago truncatula*. Sci. Rep. **8**:2046. https://doi.org/10.1038/s41598-018-20359-4.

Larrainzar, E., Riely, B.K., Kim, S.C., Carrasquilla-Garcia, N., Yu, H.J., Hwang, H.J., Oh, M., Kim, G.B., Surendrarao, A.K., Chasman, D., et al. (2015). Deep sequencing of the *Medicago truncatula* root transcriptome reveals a massive and early interaction between nodulation factor and ethylene signals. Plant Physiol. **169**:233–265. https://doi.org/10.1104/pp.15.00350.

Libault, M., Govindarajulu, M., Berg, R.H., Ong, Y.T., Puricelli, K., Taylor, C.G., Xu, D., and Stacey, G. (2011). A dual-targeted soybean protein is involved in *Bradyrhizobium japonicum* infection of soybean root hair and cortical cells. Mol. Plant Microbe Interact. **24**:1051–1060. https://doi.org/10.1094/mpmi-12-10-0281.

Libault, M., Farmer, A., Brechenmacher, L., Drnevich, J., Langley, R.J., Bilgin, D.D., Radwan, O., Neece, D.J., Clough, S.J., May, G.D., et al. (2009). Complete transcriptome of the soybean root hair cell, a single-cell model, and its alteration in response to *Bradyrhizobium japonicum* infection. Plant Physiol. **152**:541–552. https://doi.org/10.1104/pp.109.148379.

Limpens, E., Ivanov, S., van Esse, W., Voets, G., Fedorova, E., and Bisseling, T. (2009). Medicago N2-fixing symbiosomes acquire the endocytic identity marker Rab7 but delay the acquisition of vacuolar identity. Plant Cell **21**:2811–2828. https://doi.org/10.1105/tpc.108.064410.

Lin, J., Roswanjaya, Y.P., Kohlen, W., Stougaard, J., and Reid, D. (2021). Nitrate restricts nodule organogenesis through inhibition of cytokinin biosynthesis in *Lotus japonicus*. Nat. Commun. **12**:6544. https://doi.org/10.1038/s41467-021-26820-9.

Liu, C.-W., Breakspear, A., Stacey, N., Findlay, K., Nakashima, J., Ramakrishnan, K., Liu, M., Xie, F., Endre, G., de Carvalho-Niebel, F., et al. (2019a). A protein complex required for polar growth of rhizobial infection threads. Nat. Commun. **10**:2848. https://doi.org/10.1038/s41467-019-10029-y.

Liu, C.-W., Breakspear, A., Guan, D., Cerri, M.R., Jackson, K., Jiang, S., Robson, F., Radhakrishnan, G.V., Roy, S., Bone, C., et al. (2019b). NIN acts as a network hub controlling a growth module required for rhizobial infection. Plant Physiol. **179**:1704–1722. https://doi.org/10.1104/pp.18.01572.

Liu, J., Deng, J., Zhu, F., Li, Y., Lu, Z., Qin, P., Wang, T., and Dong, J. (2018). The MtDMI2-MtPUB2 negative Feedback loop plays a role in nodulation homeostasis. Plant Physiol. **176**:3003–3026. https://doi.org/10.1104/pp.17.01587.

Liu, Q., Liang, Z., Feng, D., Jiang, S., Wang, Y., Du, Z., Li, R., Hu, G., Zhang, P., Ma, Y., et al. (2021). Transcriptional landscape of rice roots at the single-cell resolution. Mol. Plant **14**:384–394. https://doi.org/10.1016/j.molp.2020.12.014.

Liu, W., Kohlen, W., Lillo, A., Op den Camp, R., Ivanov, S., Hartog, M., Limpens, E., Jamil, M., Smaczniak, C., Kaufmann, K., et al. (2011). Strigolactone biosynthesis in *Medicago truncatula* and rice requires the symbiotic GRAS-type transcription factors NSP1 and NSP2. Plant Cell **23**:3853–3865. https://doi.org/10.1105/tpc.111.089771.

Lohar, D.P., Sharopova, N., Endre, G., Penuela, S., Samac, D., Town, C., Silverstein, K.A.T., and VandenBosch, K.A. (2005). Transcript analysis of early nodulation events in *Medicago truncatula*. Plant Physiol. **140**:221–234. https://doi.org/10.1104/pp.105.070326.

Luo, Z., Lin, J.-s., Zhu, Y., Fu, M., Li, X., and Xie, F. (2021). NLP1 reciprocally regulates nitrate inhibition of nodulation through SUNN-CRA2 signaling in *Medicago truncatula*. Plant Commun. **2**:100183. https://doi.org/10.1016/j.xplc.2021.100183.

Lyons, E., and Freeling, M. (2008). How to usefully compare homologous plant genes and chromosomes as DNA sequences. Plant J. **53**:661–673. https://doi.org/10.1111/j.1365-313X.2007.03326.x.

Lyons, E., Pedersen, B., Kane, J., Alam, M., Ming, R., Tang, H., Wang, X., Bowers, J., Paterson, A., Lisch, D., et al. (2008). Finding and comparing syntenic regions among Arabidopsis and the outgroups papaya, poplar, and grape: CoGe with rosids. Plant Physiology **148**:1772–1781. https://doi.org/10.1104/pp.108.124867.

Makabe, S., Yamori, W., Kong, K., Niimi, H., and Nakamura, I. (2017). Expression of rice 45S rRNA promotes cell proliferation, leading to enhancement of growth in transgenic tobacco. Plant Biotechnol. **34**:29–38. https://doi.org/10.5511/plantbiotechnology.17.0216a.

Marino, D., Andrio, E., Danchin, E.G.J., Oger, E., Gucciardo, S., Lambert, A., Puppo, A., and Pauly, N. (2011). A *Medicago truncatula* NADPH oxidase is involved in symbiotic nodule functioning. New Phytol. **189**:580–592. https://doi.org/10.1111/j.1469-8137.2010.03509.x.

Mbengue, M., Camut, S., de Carvalho-Niebel, F., Deslandes, L., Froidure, S., Klaus-Heisen, D., Moreau, S., Rivas, S., Timmers, T., Hervé, C., et al. (2010). The *Medicago truncatula* E3 ubiquitin ligase PUB1 interacts with the LYK3 symbiotic receptor and negatively regulates infection and nodulation. Plant Cell **22**:3474–3488. https://doi.org/10.1105/tpc.110.075861.

Mergaert, P., Kereszt, A., and Kondorosi, E. (2019). Gene expression in nitrogen-fixing symbiotic nodule cells in *Medicago truncatula* and other nodulating plants. Plant Cell **32**:42–68. https://doi.org/10.1105/tpc.19.00494.

Messinese, E., Mun, J.H., Yeun, L.H., Jayaraman, D., Rougé, P., Barre, A., Lougnon, G., Schornack, S., Bono, J.J., Cook, D.R., et al. (2007). A novel nuclear protein interacts with the symbiotic DMI3 calcium- and calmodulin-dependent protein kinase of *Medicago truncatula*. Mol. Plant Microbe Interact. **20**:912–921. https://doi.org/10.1094/mpmi-20-8-0912.

Miao, Z., Deng, K., Wang, X., and Zhang, X. (2018). DEsingle for detecting three types of differential expression in single-cell RNA-seq data. Bioinformatics **34**:3223–3224. https://doi.org/10.1093/bioinformatics/bty332.

Middleton, P.H., Jakab, J., Penmetsa, R.V., Starker, C.G., Doll, J., Kaló, P., Prabhu, R., Marsh, J.F., Mitra, R.M., Kereszt, A., et al.

(2007). An ERF transcription factor in *Medicago truncatula* that is essential for Nod factor signal transduction. Plant Cell **19**:1221–1234. https://doi.org/10.1105/tpc.106.048264.

Mohd-Radzman, N.A., Laffont, C., Ivanovici, A., Patel, N., Reid, D., Stougaard, J., Frugier, F., Imin, N., and Djordjevic, M.A. (2016). Different pathways act downstream of the CEP peptide receptor CRA2 to regulate lateral root and nodule development. Plant Physiol **171**:2536–2548. https://doi.org/10.1104/pp.16.00113.

Montiel, J., Fonseca-García, C., and Quinto, C. (2018). Phylogeny and expression of NADPH oxidases during symbiotic nodule formation. Agriculture **8**:179.

Montiel, J., Arthikala, M.K., Cárdenas, L., and Quinto, C. (2016). Legume NADPH oxidases have crucial roles at different stages of nodulation. Int. J. Mol. Sci. **17**. https://doi.org/10.3390/ijms17050680.

Müller, L.M., Flokova, K., Schnabel, E., Sun, X., Fei, Z., Frugoli, J., Bouwmeester, H.J., and Harrison, M.J. (2019). A CLE-SUNN module regulates strigolactone content and fungal colonization in arbuscular mycorrhiza. Nat Plants **5**:933–939. https://doi.org/10.1038/s41477-019-0501-1.

Murray, J.D., Karas, B.J., Sato, S., Tabata, S., Amyot, L., and Szczyglowski, K. (2007). A cytokinin perception mutant colonized by Rhizobium in the absence of nodule organogenesis. Science **315**:101–104. https://doi.org/10.1126/science.1132514.

Murray, J.D., Muni, R.R., Torres-Jerez, I., Tang, Y., Allen, S., Andriankaja, M., Li, G., Laxmi, A., Cheng, X., Wen, J., et al. (2011). Vapyrin, a gene essential for intracellular progression of arbuscular mycorrhizal symbiosis, is also essential for infection by rhizobia in the nodule symbiosis of *Medicago truncatula*. Plant J. **65**:244–252. https://doi.org/10.1111/j.1365-313X.2010.04415.x.

Nguyen, N.N.T., Clua, J., Vetal, P.V., Vuarambon, D.J., De Bellis, D., Pervent, M., Lepetit, M., Udvardi, M., Valentine, A.J., and Poirier, Y. (2020). PHO1 family members transport phosphate from infected nodule cells to bacteroids in Medicago truncatula. Plant Physiol. **185**:196–209. https://doi.org/10.1093/plphys/kiaa016.

Nutman, P.S. (1959). Some observations on root-hair infection by nodule bacteria. J. Exp. Bot. **10**:250–263. https://doi.org/10.1093/jxb/10.2.250.

Olvera-Carrillo, Y., Van Bel, M., Van Hautegem, T., Fendrych, M., Huysmans, M., Simaskova, M., van Durme, M., Buscaill, P., Rivas, S., Coll, N.S., et al. (2015). A conserved core of programmed cell death indicator genes discriminates developmentally and environmentally induced programmed cell death in plants. Plant Physiol. **169**:2684–2699. https://doi.org/10.1104/pp.15.00769.

Ouyang, J.F., Kamaraj, U.S., Cao, E.Y., and Rackham, O.J.L. (2021). ShinyCell: simple and sharable visualization of single-cell gene expression data. Bioinformatics **37**:3374–3376. https://doi.org/10.1093/bioinformatics/btab209.

Pan, H., Oztas, O., Zhang, X., Wu, X., Stonoha, C., Wang, E., Wang, B., and Wang, D. (2016). A symbiotic SNARE protein generated by alternative termination of transcription. Nature Plants **2**:15197. https://doi.org/10.1038/nplants.2015.197.

Pawela, A., Banasiak, J., Biała, W., Martinoia, E., and Jasiński, M. (2019). MtABCG20 is an ABA exporter influencing root morphology and seed germination of *Medicago truncatula*. Plant J. **98**:511–523. https://doi.org/10.1111/tpj.14234.

Pecrix, Y., Staton, S.E., Sallet, E., Lelandais-Brière, C., Moreau, S., Carrère, S., Blein, T., Jardinaud, M.-F., Latrasse, D., Zouine, M., et al. (2018). Whole-genome landscape of *Medicago truncatula* symbiotic genes. Nat Plants **4**:1017–1025. https://doi.org/10.1038/s41477-018-0286-7.

Penmetsa, R.V., Uribe, P., Anderson, J., Lichtenzveig, J., Gish, J.C., Nam, Y.W., Engstrom, E., Xu, K., Sckisel, G., Pereira, M., et al. (2008). The *Medicago truncatula* ortholog of Arabidopsis *EIN2, sickle*, is a negative regulator of symbiotic and pathogenic microbial associations. Plant J. **55**:580–595. https://doi.org/10.1111/j.1365-313X.2008.03531.x.

Pingault, L., Zogli, P., Brooks, J., and Libault, M. (2018). Enhancing phenotyping and molecular analysis of plant root system using ultrasound aeroponic technology. Curr. Protoc. Plant Biol. **3**:e20078. https://doi.org/10.1002/cppb.20078.

Plet, J., Wasson, A., Ariel, F., Le Signor, C., Baker, D., Mathesius, U., Crespi, M., and Frugier, F. (2011). MtCRE1-dependent cytokinin signaling integrates bacterial and plant cues to coordinate symbiotic nodule organogenesis in *Medicago truncatula*. Plant J. **65**:622–633. https://doi.org/10.1111/j.1365-313X.2010.04447.x.

Ponnala, L., Wang, Y., Sun, Q., and van Wijk, K.J. (2014). Correlation of mRNA and protein abundance in the developing maize leaf. Plant J. **78**:424–440. https://doi.org/10.1111/tpj.12482.

Qiao, Z., Pingault, L., Zogli, P., Langevin, M., Rech, N., Farmer, A., and Libault, M. (2017). A comparative genomic and transcriptomic analysis at the level of isolated root hair cells reveals new conserved root hair regulatory elements. Plant Mol. Biol. **94**:641–655. https://doi.org/10.1007/s11103-017-0630-8.

Riely, B.K., He, H., Venkateshwaran, M., Sarma, B., Schraiber, J., Ané, J.M., and Cook, D.R. (2011). Identification of legume *RopGEF* gene families and characterization of a *Medicago truncatula RopGEF* mediating polar growth of root hairs. Plant J. **65**:230–243. https://doi.org/10.1111/j.1365-313X.2010.04414.x.

Roy, S., Liu, W., Nandety, R.S., Crook, A., Mysore, K.S., Pislariu, C.I., Frugoli, J., Dickstein, R., and Udvardi, M.K. (2019). Celebrating 20 Years of genetic discoveries in legume nodulation and symbiotic nitrogen fixation. Plant Cell **32**:15–41. https://doi.org/10.1105/tpc.19.00279.

Roy, S., Robson, F., Lilley, J., Liu, C.W., Cheng, X., Wen, J., Walker, S., Sun, J., Cousins, D., Bone, C., et al. (2017). *MtLAX2*, a functional homologue of the Arabidopsis auxin influx transporter AUX1, is required for nodule organogenesis. Plant Physiol. **174**:326–338. https://doi.org/10.1104/pp.16.01473.

Ryu, K.H., Huang, L., Kang, H.M., and Schiefelbein, J. (2019). Single-cell RNA sequencing resolves molecular relationships among individual plant cells. Plant Physiol. **179**:1444–1456. https://doi.org/10.1104/pp.18.01482.

Schauser, L., Roussis, A., Stiller, J., and Stougaard, J. (1999). A plant regulator controlling development of symbiotic root nodules. Nature **402**:191–195. https://doi.org/10.1038/46058.

Schiessl, K., Lilley, J.L.S., Lee, T., Tamvakis, I., Kohlen, W., Bailey, P.C., Thomas, A., Luptak, J., Ramakrishnan, K., Carpenter, M.D., et al. (2019). NODULE INCEPTION recruits the lateral root developmental program for symbiotic nodule organogenesis in *Medicago truncatula*. Curr. Biol. **29**:3657–3668.e5. https://doi.org/10.1016/j.cub.2019.09.005.

Schnabel, E., Karve, A., Kassaw, T., Mukherjee, A., Zhou, X., Hall, T., and Frugoli, J. (2012). The *M. truncatula SUNN* gene is expressed in vascular tissue, similarly to *RDN1*, consistent with the role of these nodulation regulation genes in long distance signaling. Plant Signal. Behav. **7**:4–6. https://doi.org/10.4161/psb.7.1.18491.

Schnabel, E.L., Kassaw, T.K., Smith, L.S., Marsh, J.F., Oldroyd, G.E., Long, S.R., and Frugoli, J.A. (2011). The *ROOT DETERMINED NODULATION1* gene regulates nodule number in roots of *Medicago truncatula* and defines a highly conserved, uncharacterized plant gene family. Plant Physiol. **157**:328–340. https://doi.org/10.1104/pp.111.178756.

Schwacke, R., Ponce-Soto, G.Y., Krause, K., Bolger, A.M., Arsova, B., Hallab, A., Gruden, K., Stitt, M., Bolger, M.E., and Usadel, B. (2019). MapMan4: a refined protein classification and annotation Framework

applicable to multi-omics data analysis. Mol. Plant **12**:879–892. https://doi.org/10.1016/j.molp.2019.01.003.

Shen, C., Yue, R., Sun, T., Zhang, L., Xu, L., Tie, S., Wang, H., and Yang, Y. (2015). Genome-wide identification and expression analysis of auxin response factor gene family in *Medicago truncatula*. Front. Plant Sci. **6**:73. https://doi.org/10.3389/fpls.2015.00073.

Shen, D., Kulikova, O., Guhl, K., Franssen, H., Kohlen, W., Bisseling, T., and Geurts, R. (2019). The *Medicago truncatula* nodule identity gene *MtNOOT1* is required for coordinated apical-basal development of the root. BMC Plant Biol. **19**:571. https://doi.org/10.1186/s12870-019-2194-z.

Shulse, C.N., Cole, B.J., Ciobanu, D., Lin, J., Yoshinaga, Y., Gouran, M., Turco, G.M., Zhu, Y., O'Malley, R.C., Brady, S.M., et al. (2019). High-throughput single-cell transcriptome profiling of plant cell types. Cell Rep. **27**:2241–2247.e4. https://doi.org/10.1016/j.celrep.2019.04.054.

Si, Z., Yang, Q., Liang, R., Chen, L., Chen, D., and Li, Y. (2019). Digalactosyldiacylglycerol synthase gene *MtDGD1* plays an essential role in nodule development and nitrogen fixation. Mol. Plant Microbe Interact. **32**:1196–1209. https://doi.org/10.1094/mpmi-11-18-0322-r.

Sinharoy, S., Torres-Jerez, I., Bandyopadhyay, K., Kereszt, A., Pislariu, C.I., Nakashima, J., Benedito, V.A., Kondorosi, E., and Udvardi, M.K. (2013). The C2H2 transcription factor regulator of symbiosome differentiation represses transcription of the secretory pathway gene VAMP721a and promotes symbiosome development in *Medicago truncatula*. Plant Cell **25**:3584–3601. https://doi.org/10.1105/tpc.113.114017.

Sinharoy, S., Liu, C., Breakspear, A., Guan, D., Shailes, S., Nakashima, J., Zhang, S., Wen, J., Torres-Jerez, I., Oldroyd, G., et al. (2016). A *Medicago truncatula* cystathionine-β-synthase-like domain-containing protein is required for rhizobial infection and symbiotic nitrogen fixation. Plant Physiol. **170**:2204–2217. https://doi.org/10.1104/pp.15.01853.

Smit, P., Raedts, J., Portyanko, V., Debellé, F., Gough, C., Bisseling, T., and Geurts, R. (2005). NSP1 of the GRAS protein family is essential for rhizobial Nod factor-induced transcription. Science **308**:1789–1791. https://doi.org/10.1126/science.1111025.

Smit, P., Limpens, E., Geurts, R., Fedorova, E., Dolgikh, E., Gough, C., and Bisseling, T. (2007). Medicago LYK3, an entry receptor in rhizobial nodulation factor signaling. Plant Physiol. **145**:183–191. https://doi.org/10.1104/pp.107.100495.

Soyano, T., Shimoda, Y., Kawaguchi, M., and Hayashi, M. (2019). A shared gene drives lateral root development and root nodule symbiosis pathways in Lotus. Science **366**:1021–1023. https://doi.org/10.1126/science.aax2153.

Suzaki, T., Kim, C.S., Takeda, N., Szczyglowski, K., and Kawaguchi, M. (2013). TRICOT encodes an AMP1-related carboxypeptidase that regulates root nodule development and shoot apical meristem maintenance in *Lotus japonicus*. Development (Cambridge, England) **140**:353–361. https://doi.org/10.1242/dev.089631.

Tan, S., Debellé, F., Gamas, P., Frugier, F., and Brault, M. (2019). Diversification of cytokinin phosphotransfer signaling genes in *Medicago truncatula* and other legume genomes. BMC Genom. **20**:373. https://doi.org/10.1186/s12864-019-5724-z.

Tavormina, P., De Coninck, B., Nikonorova, N., De Smet, I., and Cammue, B.P.A. (2015). The plant peptidome: an expanding repertoire of structural features and biological functions. Plant Cell **27**:2095–2118. https://doi.org/10.1105/tpc.15.00440.

Tellstrom, V., Usadel, B.r., Thimm, O., Stitt, M., Kuster, H., and Niehaus, K. (2007). The lipopolysaccharide of *Sinorhizobium meliloti* suppresses defense-associated gene expression in cell cultures of the host plant *Medicago truncatula*. Plant Physiol. **143**:825–837. https://doi.org/10.1104/pp.106.090985.

Thibivilliers, S., Anderson, D., and Libault, M. (2020). Isolation of plant root nuclei for single cell RNA sequencing. Curr. Prot. Plant Biol. **5**:e20120. https://doi.org/10.1002/cppb.20120.

Thimm, O., Bläsing, O., Gibon, Y., Nagel, A., Meyer, S., Krüger, P., Selbig, J., Müller, L.A., Rhee, S.Y., and Stitt, M. (2004). MAPMAN: a user-driven tool to display genomics data sets onto diagrams of metabolic pathways and other biological processes. Plant J. **37**:914–939. https://doi.org/10.1111/j.1365-313x.2004.02016.x.

Tian, Y., Liu, W., Cai, J., Zhang, L.Y., Wong, K.B., Feddermann, N., Boller, T., Xie, Z.P., and Staehelin, C. (2013). The nodulation factor hydrolase of *Medicago truncatula*: characterization of an enzyme specifically cleaving rhizobial nodulation signals. Plant Physiol. **163**:1179–1190. https://doi.org/10.1104/pp.113.223966.

Turco, G.M., Rodriguez-Medina, J., Siebert, S., Han, D., Valderrama-Gómez, M., Vahldick, H., Shulse, C.N., Cole, B.J., Juliano, C.E., Dickel, D.E., et al. (2019). Molecular mechanisms driving switch behavior in xylem cell differentiation. Cell Rep. **28**:342–351.e4. https://doi.org/10.1016/j.celrep.2019.06.041.

Van de Velde, W., Zehirov, G., Szatmari, A., Debreczeny, M., Ishihara, H., Kevei, Z., Farkas, A., Mikulass, K., Nagy, A., Tiricz, H., et al. (2010). Plant peptides govern terminal differentiation of bacteria in symbiosis. Science **327**:1122–1126. https://doi.org/10.1126/science.1184057.

van Zeijl, A., Op den Camp, Rik, H.M., Deinum, E.E., Charnikhova, T., Franssen, H., Op den Camp, Huub, J.M., Bouwmeester, H., Kohlen, W., et al. (2015). Rhizobium lipo-chitooligosaccharide signaling triggers accumulation of cytokinins in *Medicago truncatula* roots. Mol. Plant **8**:1213–1226. https://doi.org/10.1016/j.molp.2015.03.010.

Venkateshwaran, M., Cosme, A., Han, L., Banba, M., Satyshur, K.A., Schleiff, E., Parniske, M., Imaizumi-Anraku, H., and Ané, J.-M. (2012). The recent evolution of a symbiotic ion channel in the legume family altered ion conductance and improved functionality in calcium signaling. Plant Cell **24**:2528–2545. https://doi.org/10.1105/tpc.112.098475.

Verdier, J., Lalanne, D., Pelletier, S., Torres-Jerez, I., Righetti, K., Bandyopadhyay, K., Leprince, O., Chatelain, E., Vu, B.L., Gouzy, J., et al. (2013). A regulatory network-based approach dissects late maturation processes related to the acquisition of desiccation tolerance and longevity of *Medicago truncatula* seeds. Plant Physiol. **163**:757–774. https://doi.org/10.1104/pp.113.222380.

Vernié, T., Moreau, S., de Billy, F., Plet, J., Combier, J.P., Rogers, C., Oldroyd, G., Frugier, F., Niebel, A., and Gamas, P. (2008). EFD Is an ERF transcription factor involved in the control of nodule number and differentiation in *Medicago truncatula*. Plant Cell **20**:2696–2713. https://doi.org/10.1105/tpc.108.059857.

Wang, D., Griffitts, J., Starker, C., Fedorova, E., Limpens, E., Ivanov, S., Bisseling, T., and Long, S. (2010). A nodule-specific protein secretory pathway required for nitrogen-fixing symbiosis. Science **327**:1126–1129. https://doi.org/10.1126/science.1184096.

Wang, J., Hou, Q., Li, P., Yang, L., Sun, X., Benedito, V.A., Wen, J., Chen, B., Mysore, K.S., and Zhao, J. (2017). Diverse functions of multidrug and toxin extrusion (MATE) transporters in citric acid efflux and metal homeostasis in *Medicago truncatula*. Plant J. **90**:79–95. https://doi.org/10.1111/tpj.13471.

Wang, T., Li, B., Nelson, C.E., and Nabavi, S. (2019). Comparative analysis of differential gene expression analysis tools for single-cell RNA sequencing data. BMC Bioinf. **20**:40. https://doi.org/10.1186/s12859-019-2599-6.

Wang, X., Wei, C., He, F., and Yang, Q. (2022). MtPT5 phosphate transporter is involved in leaf growth and phosphate accumulation of *Medicago truncatula*. Front. Plant Sci. **13**:1005895. https://doi.org/10.3389/fpls.2022.1005895.

Xiao, T.T., Schilderink, S., Moling, S., Deinum, E.E., Kondorosi, E., Franssen, H., Kulikova, O., Niebel, A., and Bisseling, T. (2014). Fate map of *Medicago truncatula* root nodules. Development **141**:3517–3528. https://doi.org/10.1242/dev.110775.

Xie, F., Murray, J.D., Kim, J., Heckmann, A.B., Edwards, A., Oldroyd, G.E.D., and Downie, J.A. (2012). Legume pectate lyase required for root infection by rhizobia. Proc. Natl. Acad. Sci. USA **109**:633–638. https://doi.org/10.1073/pnas.1113992109.

Yoon, H.J., Hossain, M.S., Held, M., Hou, H., Kehl, M., Tromas, A., Sato, S., Tabata, S., Andersen, S.U., Stougaard, J., et al. (2014). *Lotus japonicus SUNERGOS1* encodes a predicted subunit A of a DNA topoisomerase VI that is required for nodule differentiation and accommodation of rhizobial infection. Plant J. **78**:811–821. https://doi.org/10.1111/tpj.12520.

Young, M.D., and Behjati, S. (2020). SoupX removes ambient RNA contamination from droplet-based single-cell RNA sequencing data. Gigascience **10**. https://doi.org/10.1093/gigascience/giaa151.

Zeng, L., Zhang, N., Zhang, Q., Endress, P.K., Huang, J., and Ma, H. (2017). Resolution of deep eudicot phylogeny and their temporal diversification using nuclear genes from transcriptomic and genomic datasets. New Phytol. **214**:1338–1354. https://doi.org/10.1111/nph.14503.

Zhang, T.-Q., Xu, Z.-G., Shang, G.-D., and Wang, J.-W. (2019). A single-cell RNA sequencing profiles the developmental landscape of Arabidopsis root. Mol. Plant **12**:648–660. https://doi.org/10.1016/j.molp.2019.04.004.

Zhang, T.-Q., Chen, Y., Liu, Y., Lin, W.-H., and Wang, J.-W. (2021). Single-cell transcriptome atlas and chromatin accessibility landscape reveal differentiation trajectories in the rice root. Nat. Commun. **12**:2053. https://doi.org/10.1038/s41467-021-22352-4.